MENTAL STATES AND ALCOHOLISM DETECTION USING NON-STATIONARY DECOMPOSITIONS FOR EEG SIGNALS

MAJOR PROJECT

SUBMITTED IN PARTIAL FULFILLMENT OF THE REQUIREMENTS
FOR THE AWARD OF THE DEGREE
OF

MASTER OF TECHNOLOGY
IN
SIGNAL PROCESSING AND DIGITAL DESIGN

Submitted by:

P V Keshava Krishna

2K20/SPD/08

Under the supervision of

Dr. Sachin Taran

DEPARTMENT OF ELECTRONICS AND COMMUNICATION ENGINEERING
DELHI TECHNOLOGICAL UNIVERSITY
(Formerly Delhi College of Engineering)
Bawana Road, Delhi-110042

MAY 2022

DEPARTMENT OF ELECTRONICS AND COMMUNICATION ENGINEERING
DELHI TECHNOLOGICAL UNIVERSITY
(Formerly Delhi College of Engineering)
Bawana Road, Delhi-110042

CANDIDATE'S DECLARATION

I **P V Keshava Krishna** student of M.Tech (Signal Processing and Digital Design), hereby declare that the project Dissertation titled "**Mental states and Alcoholism detection using non-stationary decompositions for EEG signals**" which is submitted by me to the Department of Electronics and Communication Engineering, Delhi Technological University, Delhi in partial fulfillment of the requirement for the award of the degree of Master of Technology, is original and not copied from any source without proper citation. This work has not previously formed the basis for the award of any Degree, Diploma Associateship, Fellowship or other similar title or recognition.

Place: Delhi **P V Keshava Krishna**

Date: May 31, 2022

DEPARTMENT OF ELECTRONICS AND COMMUNICATION ENGINEERING
DELHI TECHNOLOGICAL UNIVERSITY
(Formerly Delhi College of Engineering)
Bawana Road, Delhi-110042

CERTIFICATE

I hereby certify that the Project Report titled "**Mental states and Alcoholism detection using non-stationary decompositions for EEG signals**" which is submitted by **P V Keshava Krishna**, **2K20/SPD/08** of Electronics and Communication Department, Delhi Technological University, Delhi in partial fulfillment of the requirement for the award of the degree of Master of Technology, is a record of the project work carried out by the students under my supervision. To the best of my knowledge this work has not been submitted in part or full for any Degree or Diploma to this University or elsewhere.

Place: Delhi
Date: May 31, 2022

Dr. Sachin Taran
SUPERVISOR

ACKNOWLEDGEMENT

A successful project can never be prepared by the efforts of the person to whom the project is assigned, but it also demands the help and guardianship of people who helped in completion of the project. I would like to thank all those people who have helped me in this research and inspired me during my study.

With profound sense of gratitude, I thank Dr. Sachin Taran, my Research Supervisor, for his encouragement, support, patience and his guidance in this thesis work. Their kind comments and guidance let me complete this study in an improved manner.

I take immense delight in extending my acknowledgement to my family and friends who have been supporting me morally to keep going with this study and inspired me to come up with the expected results throughout this research work.

P V Keshava Krishna

ABSTRACT

An electroencephalogram (EEG) is an electrical signal that captures brain impulses by arranging electrodes in a specific pattern. The process of collecting EEG can be either invasive or non-invasive. Non-invasive EEG recordings are obtained from the electrodes attached to the scalp area, whereas invasive EEG recordings are obtained from the electrodes implanted into the brain, which needs surgery.

As a result, EEG data provide information into the participant's cognitive conditions. EEG, on the other hand, is susceptible to electrical noise and is best used in controlled lab circumstances rather than in real-world scenarios. Non-invasive EEG devices are becoming popular among researchers, and they are most widely used brain signal methods. The non-invasive nature of EEG-based techniques makes it more viable for the following reasons: EEG is a fast and safe way of checking brain activity, EEG approaches are non-invasive, EEG detects brain activity at a resolution of milliseconds with high precision. EEG has a less error probability, convenient to use and less setup cost with minimal danger.

The advancements in technology have bought lots of changes in human life. All the changes have reduced the efforts of humans in doing any work. The advancements reduce the mental attention level of human beings which can be dangerous in attention-seeking applications. In this work, a brain-computer interface (BCI) system is suggested for mental attention detection using EEG. To detect mental states a signal processing and machine learning-based algorithm is proposed. Flexible Analytic Wavelet Transform (FAWT) explores for feature extraction from EEG and different machine learning algorithms are tested with extracted features to detect mental states.

Initially, multiple FAWT based features are extracted out of which the log energy entropy provides the best classification performance with an optimizable k-nearest neighbor classifier. The classification performance of the proposed work has better results as compared to other similar approaches.

Alcohol consumption alters the functionality of nervous system by disturbing the neuron process, which leads to the behavioral changes in a human life. An automatic identification of alcoholics can address these issues. EEG is a widely used tool for monitoring the brain activities. In this study, singular spectrum analysis (SSA) and machine learning-based algorithm is proposed for the automatic detection of normal and alcohol EEG signals. Kruskal Wallis test is performed as a part of a statistical study and the features which satisfy $p<0.05$ are considered in the classification. Initially, multiple SSA-based features are extracted out of which the inter-quartile range and wavelength provide the best classification performance with an optimizable support vector machine classifier. The achieved classification accuracy is 94.2%.

EEG finds various applications in the identification and diagnosis of neurological diseases and brain computer interface. BCI is a system works on the instructions given by the human brain and helps the disabled to communicate with surroundings. Alcoholism is one of the leading causes of disease and can be identified and diagnosed by using the EEG signals which can avoid road accidents.

To explore the complexity of the EEG signals the signal processing in machine learning tools are employed. Various non-stationary tools are employed for the decomposition of EEG signals and multiple features are extracted. The extracted features are further tested with various machine learning algorithms for the classification of EEG signal.

CONTENTS

LIST OF FIGS

List of Tables

List of Symbols and Abbreviations

BCI: Brain Computer Interface

EEG: Electroencephalogram

FAWT: Flexible Analytic Wavelet Transform

KW: Kruskal Wallis

MI: Motor Imagery

DT: Decision Tree

CSP: Common Spatial Pattern

SVM: Support Vector Machine

LDA: Linear Discriminant Analysis

KNN: k-nearest Neighbor

STFT: Short Time Fourier Transform

RDWT: Rational dilation wavelet transform

DA: Discriminant Analysis

LEE: Log Energy Entropy

IQR: Inter Quartile Range

WAVELEN: Waveform Length

SSA: Singular Spectrum Analysis

EOG: Electrooculography

MRI: Magnetic resonance imaging

ECG: Electrocardiography

MEG: Magnetoencephalography

FMRI: Functional magnetic resonance imaging

PET: A positron emission tomography

NIRS: Near-infrared spectroscopy

EROS: Elaboration Of Reactions For Organic Synthesis

EMD: Empirical Mode Decomposition

EWT: Empirical Wavelet Transform

ICA: Independent Component Analysis

FFT: Fast Fourier Transform

AR: Auto Regressive

WPD: Wavelet Packet Decomposition

PCA: Principle Component Analysis

PSD: Power Spectral Density

TQWT: Tunable Q Wavelet Transform

CHAPTER 1
INTRODUCTION

1.1 Human Brain

Human brains are the most complicated organs on the planet. It is in charge of a variety of physical tasks. It has a 10 billion nerve cells and neurons brain network. Human sensations, hunger, thirst, physical movements, and sleep are all handled by it. It is in charge of nearly all of a human's essential actions for existence. It sends and receives signals to communicate with the environment of the body part. The brainstem, spinal cord, and big brain are all part of the central nervous system, as shown in Fig. 1.1. The brainstem connects the spinal cord with the big brain. Based on its anatomy and functions, it is separated into three components.

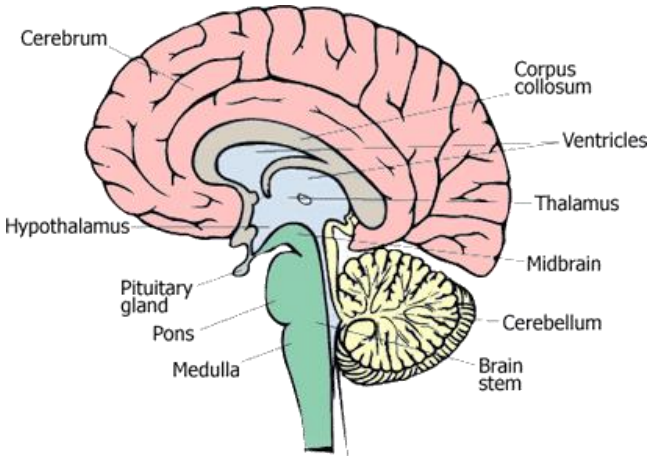

Fig. 1.1. Various regions of Human Brain [1].

1.2 Brain Structure

Based on anatomy, the brain is divided into three regions: the rear brain, the midbrain, and the forebrain. The cerebellum and fourth ventricle, as well as the spinal cord, are located above the myelencephalon in the back brain. In the second segment of the mesencephalon, which exits in the midbrain, are the tectum, tegmentum, and cerebral aqueduct. In the third segment, the diencephalon and telencephalon leave the forebrain [1].

Based on its functions, the brain is divided into three parts. The forebrain, also known as the cerebrum or large brain, is the first component and is in charge of higher-level mental tasks including calculation. The second part of the brainstem is in charge of visual functions. The third section, the cerebellum, is in control of physical movements.

1.3 Electroencephalography (EEG)

Human brain is a collection of several number of neurons, which shows high resolution of spatio-temporal dynamics. For recording the data, there are many techniques such as MRI, EEG, MEG, FMRI, PET, NIRS, EROS. Among these EEG is the most prominent technique that is used due to the measure of control activity with the temporal resolution with which less than millisecond is provided using each signal. This signal is also used for extracting the features in the brain signal.

The first EEG signal is being recorded by Hans Bazar in 1929 in past there are some limitations that are subjected to visual only. The visible review is extremely subjective and hardly permits any applied math analysis. These ways are terribly dull and Time consumption is also high.

So basically, EEG data will be of nonlinear, non-gaussian, non-correlated or a random signal. using EEG signal some kind of injuries or brain diseases can be detected which are related to neurology, and sleep disorder like Narcolepsy, tumor, depression and many other issues which relate with stress. Signal Processing can differentiate a normal and abnormal person using their brain activity.

The electrical impulses are generated by the neurons for communication between other neurons. The electrodes are used for collecting EEG data. They are placed on the scalp of measuring the amplitude of the impulses which are generated by neurons. EEG signal frequency ranges from one Hertz to hundred Hertz, among them hundred Hertz is used very rarely. The range of amplitude varies between 10 microvolts to 100 microvolts.

Any evoked reaction that is imbedded at intervals on going background activities has a poor signal-to-noise ratio in the collected signal. This eliminates a variety of activities from the data collection process, such as eye blinking, muscle activity, and other background activities. As a result, these signals are captured in low-noise environments and using complex machinery that are free of interference and a variety of disturbances.

Other than poor spatial resolution EEG are good in temporal resolution which is less than one milli-second. this signal has very low frequency in terms of Hertz. Their classification is done based on the frequency groups that are classified as Delta, theta, alpha, beta and gamma based on their emotion’s amplitude is being varied.

The EEG is a signal that represents brain activity. The signal waves include crucial information about the brain's condition. It is a non-invasive technology for brain imaging that records electrical potentials on the scalp's surface as a result of the electrical activity of large groups of neurons in the brain [2]. Non-invasive means that the body is not invaded or sliced open, as it would be during surgical examinations or therapeutic surgery. Non-invasive approach is the polar opposite of intrusive procedure.

Fig. 1.2. An EEG recording headset [3].

1.4 Types of Signals

EEG signals are complex signals that are described in terms of rhythmic and transient signals, as seen in Fig. 1.3. Different frequency bands are used to divide the rhythmic action. When EEG signals are captured in different states, such as doing a task or relaxing, different persons of different ages may have varying magnitude and frequency ranges.

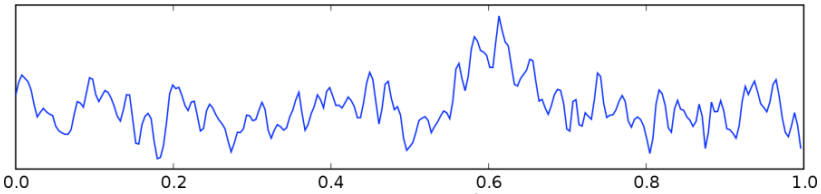

Fig. 1.3. A representation of EEG Signals [4].

Five types of waves may be distinguished based on frequency ranges. From low to high frequency, they are alpha (α), theta (θ), beta (β), delta (δ), and gamma (γ) accordingly.

A specific wave is mostly available in specific lobe of cerebral cortex however this is not always true.

1.4.1 Delta Waves (δ)

The frequency range of delta waves is 0–4 Hz. Deep sleep, coma, as well as being conscious, are all mental condition connected with these frequency range. It is usually regarded a clinical phenomenon in the waking state. The greater the magnitude, the more severe the problem being evaluated. These rages of waves are less as you get older, but they're still present in healthy people when they're awake.

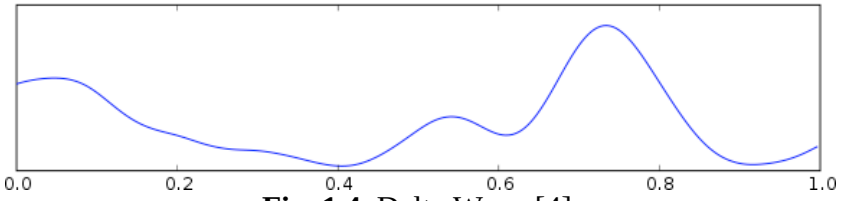

Fig. 1.4. Delta Wave [4].

1.4.2 Theta Waves (θ)

Theta waves have a frequency between 4 and 8 Hz. Boosting ideas, creative ideology, and sleepy materials are all mental attentions connected with these waves. These waves appear in the head's central, temporal, and parietal regions. These waves are common in healthy persons when they are sleeping deeply.

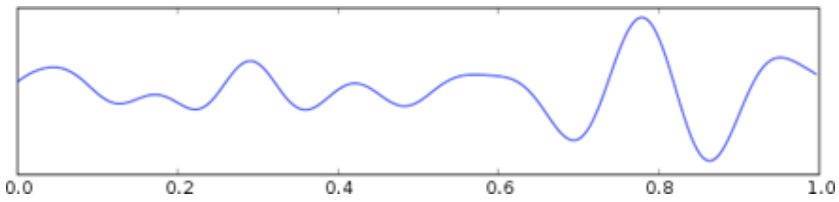

Fig. 1.5. Theta Wave [4].

1.4.3 Alpha Waves (α)

Alpha waves have a frequency between 8 and 13 Hz. Relaxed and peaceful mental states are related with these waves. These frequency range appear on the back of the skull and in the occipital region of the brain. In comparison to other waves, these have a large amplitude. While the person is awake and clam, this can be noticed. These waves might sometimes disrupt the -rhythm. These ranges are typically seen in people who are calm and relaxed while awake.

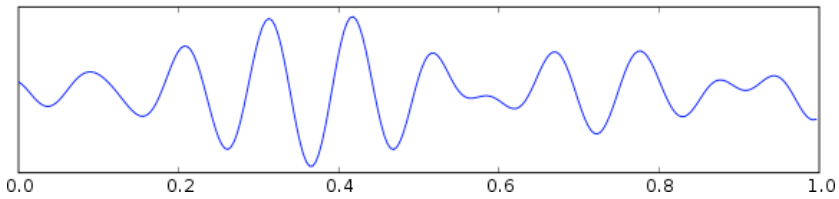

Fig. 1.6. Alpha Wave [4].

1.4.4 Beta Waves (β)

Beta waves have a frequency between 13 and 30 Hz. Highly concentrated and attentive mental states, such as intense thinking and concentration, are connected with these waves. In comparison to other waves, beta waves have a wide frequency range. These waves appear on the front side of the skull and in the brain's core center.

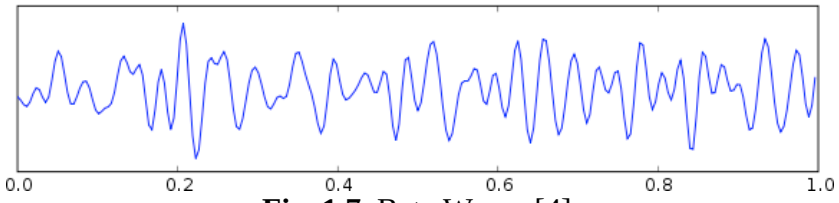

Fig. 1.7. Beta Waves [4].

1.4.5 Gamma Waves (γ)

Gamma waves have a frequency of less than 30 Hz. Parallelly work and multi-tasking are mental states related with this. Because of their small magnitudes, these waves are difficult to discern. These waves can be found in every area of the brain.

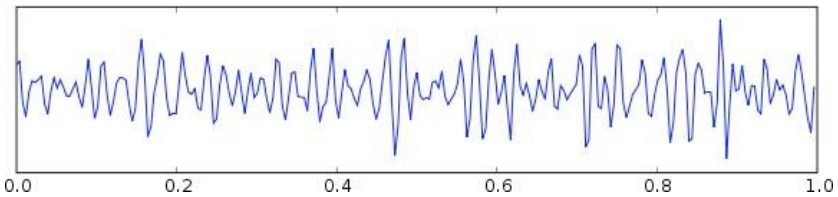

Fig. 1.8. Gamma Waves [4].

1.5 Acquirement of EEG Signals

Sculp is used to collect EEG signals. Electrodes attached to the head are used to measure the signals. The basic premise of EEG is to calculate the voltage difference between two or more electrodes. Either the mastoids or the ear lobes have one or more electrodes connected to them. Reference electrodes are what they're called. These electrodes aid in the detection of the skull's background electric field. The placement of reference electrodes is critical. They should not be placed near the brain or in any other area of the body because signals may be altered by muscle or heart electrical activity [5].

Fig. 1.9. An EEG signal acquisition headset with electrodes [3].

Various EEG devices are available, each with a different number of electrodes and filters. These devices assist in the acquisition of analogue EEG signals, which are subsequently converted to digital data with a sampling frequency. Filters aid in the removal of artefacts. By deleting signals like Electromyography (EMG) and Electrocardiography (ECG), unwanted frequencies are disregarded using low pass and high pass filters [6]. During data processing, the data resolution is also crucial. As a result, while recording EEG data, sample frequency, sampling rate, and the number of electrodes is all critical considerations.

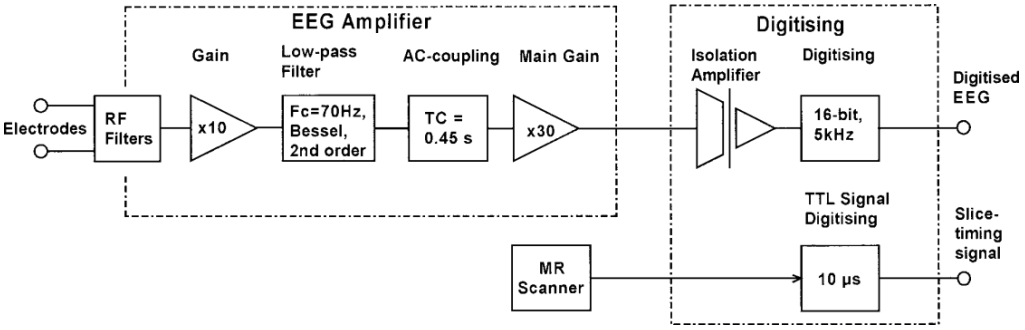

Fig. 1.10. The EEG recording system building blocks [7].

Various electrodes are used to access EEG signal using various methods. Some of the electrodes used for recording EEG data are:

- Reusable Electrodes.
- Disposable Electrodes.
- Electrodes Caps.
- Saline-Based Electrodes.
- Needle Electrodes.

1.6 Artifacts

The Artifacts are undesirable signals caused by noise in electronic circuits, for example. These are not caused by brain activity, but rather by signal measurement issues that make analysis challenging.

Artifacts come in a variety of shapes and sizes. One of the primary abnormalities is due to the system's impedance, and another is a sampling frequency artefact induced by the ground loop, which is 50 Hz and 60 Hz. The significance of artefacts and their removal can be better understood by looking at Fig. 1.11:

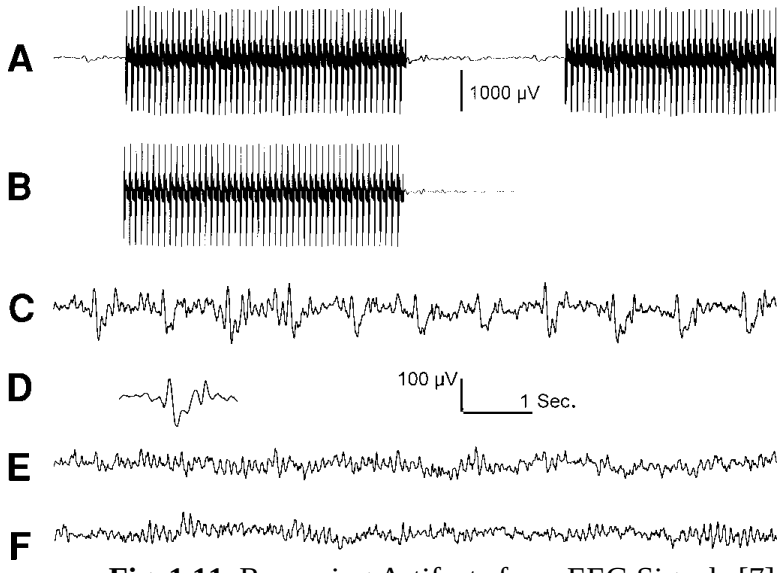

Fig. 1.11. Removing Artifacts from EEG Signals [7].

(A) A raw EEG data with artifacts.

(B) The averaged imaging artifact.

(C) The outcome of eliminating the averaged image artefact from the EEG in A, then down sampling and displaying Pulse artefact.

(D) The averaged pulse artifact from trace C (not to scale).

(E) Result of subtracting the averaged pulse artifact in D from the EEG in C.

(F) The EEG from the same subject, recorded outside the scanner, i.e., free of imaging and pulse artifact. The character of this EEG appears to match closely the artifact corrected trace in E.

However, some of the artifacts are useful. Biological signals such as EMG and EKG can help to predict different mental states. Such as, EMG artifact which is due to eye blinking can provide information about sleep or awake states.

10-20 System of Electrodes Placement

One of the commonly used methods of electrode placement is the 10-20 System for recording EEG signals which is standardized by the American Electroencephalographic Society. Using this system, a total of 21 electrodes are placed on the scalp as shown in A of Fig. 1The location ion of placement for electrodes is as:

Nasion: Electrodes placed at the level of eyes and top of nose are Reference Points, Nasion. Inion: Electrodes placed on the middle back side backside of head and base of skull are inion.

The above points are used to calculate the dimensions of the skull. The locations of electrodes are selected by dividing parameters into 10% and 20% increments. As shown in B of Fig. 1.9 [8], three electrodes are inserted in the midst of adjacent spots. The 10-20 system is based on the relationship between the placement of an electrode and the cerebral cortex. The following electrode letters are used to decide the placements:

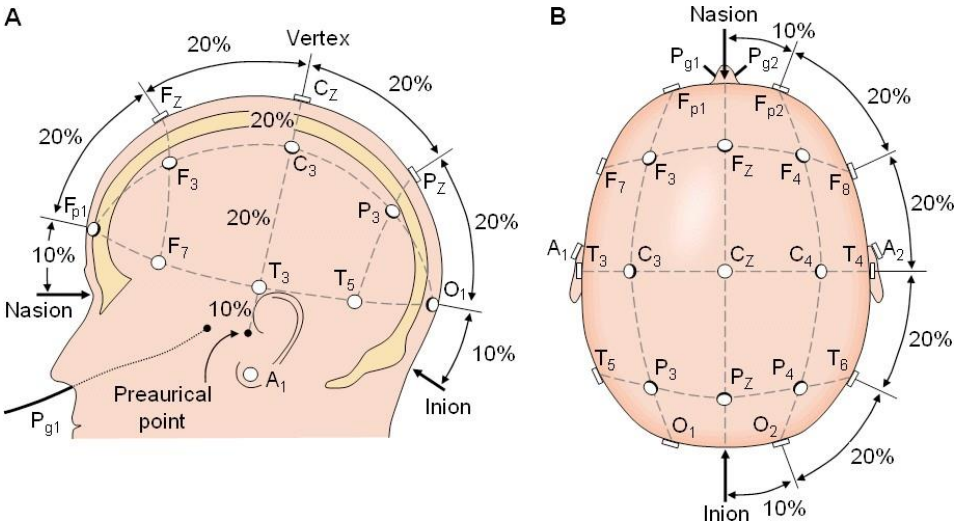

Fig. 1.12. 10-20 System of Electrodes Placement [8] Seen from (A) Left and (B) Above the Head. Here A stands for ear lobe, C stands for central lobe, F stands for frontal lobe, F_p stands for frontal polar, O stands for occipital lobe, P_g stands for nasopharyngeal and T stands for temporal lobe.

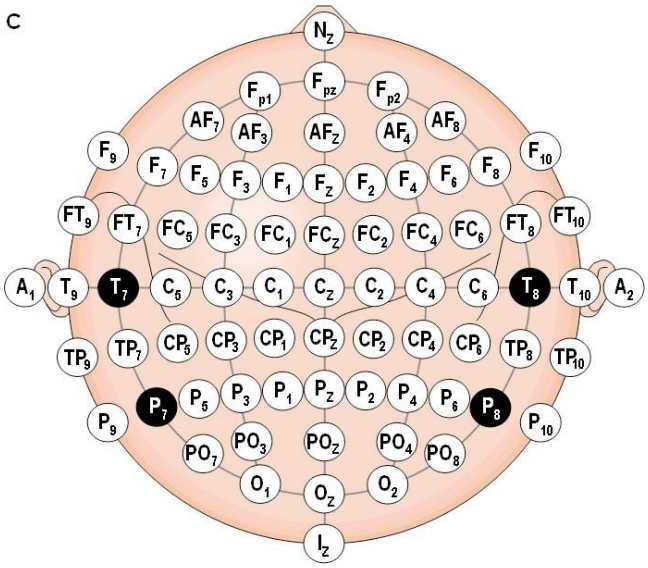

Fig. 1.13. Location and Nomenclature of the Intermediate 10% Electrodes [8].

There are several additional ways for recording EEG signals than the 10-20 system. For recording electric potentials on the scalp, the Queen Square technique of electrode placement was proposed as a standard [8]. Bipolar or unipolar electrodes can be used to provide EEG measurements. In bipolar, the difference in potential between two electrodes is measured, but in unipolar, the average of all electrodes is compared to the potential of each electrode [8].

1.7 Problem Background and Motivation:

EEG signals have various applications in the identification of sleep apnea, Alcoholism, Brain-computer interface (BCI) [9, 54, 39]. This work presents the classification of alcoholism and BCI. The study of human-computer interaction is known as a BCI. BCI aspires to create a design that achieves a good fit between the user, the machine, and the needed services in order to reach a particular level of quality and optimality in the services. BCI is now one of the most active research fields in the field of computer science. Modern forms of human-driven and human-centric contact with digital media have opened up new avenues for modernizing various aspects of human existence, such as learning and working. Because emotions are so important in people's daily lives, BCI applications have enhanced the importance of emotion identification. BCI is the source of communication for

the disabled people. The successful classification of various motor imagery (MI) tasks finds various application towards disabled people in driving applications, medical applications.

The alcoholism is the other problem focused. The early identification of alcoholism can prevent accidents and several hazards. Drinking leads to the third position in diseases. Alcoholism-related genetic diseases include weaker and less organized theta rhythms. Drinking is the third major cause of disease as per the world health organization. Furthermore, alcoholism increases as per disability-adjusted life-years (DALY) which estimates that 5.1% of global diseases are related with alcohol consumption. Furthermore, the rising incidence of malignancies linked with alcohol adds to the seriousness of the situation.

1.8 Objectives:

1. Need of non-stationary methods for EEG signals analysis and classification.
2. Need of non-stationary methods for the classification of MI tasks in BCI applications.
3. Need of feature extraction methods for the classification of normal and alcoholics EEG signals.

CHAPTER 2

Classification of Mental Attention States EEG Using Analytic Wavelet Transform and Optimizable k-nearest Neighbors

2.1 Introduction

The BCI is a system that works on human brain instructions. Various motor imagery (MI) task applications are controlled by the instructions. MI is the process of imagining a certain task in the brain. MI-based BCI discovers ways for impaired persons to engage with their surroundings [10]. BCI allows individuals to respond more quickly to changes in their environment and does not require the involvement of peripheral nerves or muscles. BCI is a non-muscular method of communicating a person's actions to external devices like computers, assistive tools, speech synthesizers, and brain prostheses. The reliability of the BCI system depends on the successful classification of MI tasks. MI classification using electroencephalogram (EEG) gives a better result due to the following reasons: EEG is a fast and safe way of checking brain activity, EEG approaches are non-invasive [11, 12], EEG detects brain activity at a resolution of milliseconds with high precision [13].

2.1.1 Literature Survey

Several studies are conducted to classify MI tasks. The Analytic features are investigated for EEG data categorization under the various MI tasks [13]. A decision tree (DT) based classification algorithm is employed for classifying computer cursor up, down, left, and right movements [14]. To classify the MI tasks a technique named Filter Bank-Tikhonov Regularization Common Spatial Pattern (CSP) Random Forest has been developed [15]. For extracting power features and MI task classification, a comparison of spectral signal representations such as power spectral density and wavelet techniques are performed [16]. A Meta-analytic review based on focusing on emotions as voluntary and stimulus-independent commands towards BCIs is explored [17].

An efficient feature selection technique based on an evolutionary algorithm is suggested to generate a subset of important features that enhances the classification accuracy [18]. Analyzing continuous EEG signals including specific cue-triggered mental states is used to investigate a framework for developing an asynchronous BCI [19]. For classifying MI tasks, a wavelet-based time-frequency analysis technique is developed [20]. For the categorization of right-left limb movement, the linear discriminant analysis (LDA), quadratic discriminant analysis (QDA), and K-nearest neighbor (KNN) algorithms are explored [21]. Wavelet packet analysis is used to investigate slow cortical potentials self-regulation. A multilayer perceptron is used to classify the EEG data [22].

A CSP and chaotic particle swarm optimization-based technique is explored for MI EEG classification with twin support vector machine (SVM) [23]. The master slave features of asynchronous BCI are explored to classify MI tasks [24]. A graphical method is suggested to model the interaction between EEG electrode recordings during left and right hands MI activities [25]. The accuracy of MI tasks is improved using a novel approach called temporally constrained sparse group spatial pattern for the optimization of the filter banks and time window along with CSP [26]. For the minimum number of channel selections, research-based on time-frequency wavelet coherence is proposed to classify the MI tasks [27].

A filtering method based on multivariate empirical mode decomposition is explored for MI tasks categorization [28]. A system based on EEG BCI that measures attention levels has been proposed. Three mental states are classified using KNN algorithms based on the self-assessment manikin model is proposed [29]. A single trail-based BCI system is suggested for monitoring the change in mental states [30]. The non-linear features and SVM are explored for the classification of mental states [31]. An SVM is used for the classification of attentive and non-attentive mental states of the students [32].

A BCI based on the robotic simulator is proposed in which wavelet function is used as the feature extraction tool and classification is performed by Recurrent Neural Networks [33]. The use of monitoring drivers to concentrate attention and engage operators in multi-tasking situations is presented [34]. A short time Fourier transform (STFT) with SVM approach is presented for mental states classification [35]. A rational dilation wavelet transforms (RDWT) with bagged trees (BT) based approach is proposed for the classification of MI tasks [36]. An empirical mode decomposition

(EMD) with multi class least square SVM (MS-LS-SVM) is explored to classify emotion EEG signals [37].

This work suggested a Flexible analytic wavelet transform (FAWT) and an optimizable classifier-based algorithm to classify mental states. EEG data is decomposed by using FAWT and features are extracted corresponding to focused, unfocused, and drowsiness EEG signals. The obtained features are driven to different classifiers for the classification of the mental state. The remaining paper is structured in the following order: In Section 2, the methodology is split into four sections: dataset, feature extraction, decomposition method, and classification. The results and discussion are presented in Section 3 and the conclusion is presented in Section 4.

2.2 Methodology

The block diagram of the presented method is shown in Fig. 2.1. Initially, the EEG signal is given as the input to FAWT for decomposition. The extracted features are further tested with various classification tools for the classification.

2.2.1 Dataset

The dataset used in this work consists of twenty-five hours of EEG recordings collected from the 5 subjects under the low-intensity control activity. The activity entailed utilizing the Microsoft-Train-Simulator application to operate a computer-simulated train. In each trial, participants were asked to use the above-mentioned computer simulation program to manage a train for 35-55 minutes. The dataset comprises of three different mental states they are focused on awareness, unfocused but awake, and drowsiness [35].

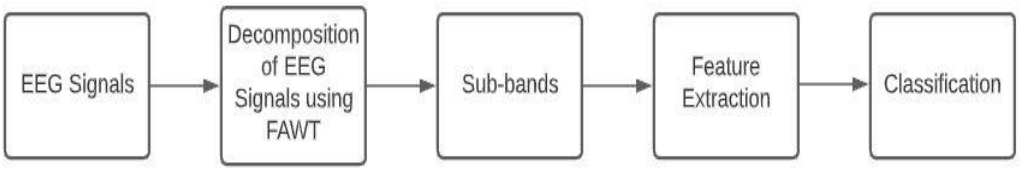

Fig. 2.1. The block diagram of the proposed model.

2.2.2 Flexible analytic wavelet transform

The flexible analytic wavelet transform (FAWT) is primarily used to investigate non-stationary signals. FAWT are analytic wavelet transforms having a wide range of frequency and temporal coverage. For the decomposition of a signal, FAWT utilizes iterative filter banks which include two high pass (HP) channels and one low pass (LP) channel. Here e and f, g and h are the LP up and down, HP up and down sampling

parameters. FAWT employs a Hilbert transform with a pair of atoms to manage redundancy(R), quality factor (Q), and dilation factor (d). The ratio of the center frequency to the bandwidth is Q, which is responsible for the frequency resolution. d determines the wavelet's size. the ratio of the input sample to the output sample is R. The parameters are defined as follows [38]:

$$R = \frac{g}{h(1-d)} \tag{2.1}$$

$$Q = \frac{2-\beta}{\beta} \tag{2.2}$$

$$d = \frac{e}{f} \tag{2.3}$$

$$\beta \leq 1 \tag{2.4}$$

$$R > \frac{\beta}{1-d} \tag{2.5}$$

The frequency response of LP filter L(ω) can be defined by the following equation [39]:

$$\mathrm{L}(\omega) = \begin{cases} \sqrt{ef}, & for \quad |\omega| < \omega_{\boldsymbol{p}} \\ \sqrt{ef}\ \theta\left(\frac{\omega-\omega_{\boldsymbol{p}}}{\omega_s-\omega_{\boldsymbol{p}}}\right), & for \quad \omega_{\boldsymbol{p}} \leq \omega \leq \omega_s \\ \sqrt{ef}\ \theta\left(\frac{\pi-\omega+\omega_{\boldsymbol{p}}}{\omega_s-\omega_{\boldsymbol{p}}}\right), & for \quad \omega_s \leq |\omega| \leq \omega_{\boldsymbol{p}} \\ 0, & for \quad |\omega| \geq \omega_s \end{cases} \tag{2.6}$$

Frequencies of the LP filter's stop band and pass band are represented by ω_s and $\omega_{\boldsymbol{p}}$, respectively.

$$\omega_{\boldsymbol{p}} = \frac{(1-\beta)\pi}{e} + \frac{\varepsilon}{e} \tag{2.7}$$

$$\omega_s = \frac{\pi}{f} \tag{2.8}$$

Likewise, the frequency response of HP filter H(ω) can be defined by the following equation [39]:

$$L(\omega) = \begin{cases} \sqrt{2gh}\ \theta\left(\frac{\pi - \omega - \omega_0}{\omega_1 - \omega_0}\right), & for \quad \omega_0 \le \omega \le \omega_1 \\ \sqrt{2gh}\ , & for \quad \omega_1 \le \omega \le \omega_2 \\ \sqrt{2gh}\,\theta\left(\frac{\omega - \omega_2}{\omega_3 - \omega_2}\right), & for \quad \omega_2 \le \omega \le \omega_3 \\ 0, & for \quad \omega \in [(0\ ,\ \omega_0) U (\omega_3\ , 2\pi)] \end{cases} \tag{2.9}$$

whereas, $\theta(\omega)$ is transition band and is represented as

$$\theta(\omega) = \left(\frac{1 + \cos(\omega)}{2}\right)\left(\sqrt{2 - \cos(\omega)}\right) \qquad for \qquad \omega \in [0\ , \pi] \tag{2.10}$$

The parameters used for decomposing an EEG signal into sub-bands are e = 3, f = 4, g= 1, h = 2, and decomposition levels are 15.

2.2.3 Feature Extraction

This paper uses FAWT for extracting the features from EEG brain activity. The log of the total number of microscopic states corresponding to a given macro-state of thermodynamics is entropy. The feature has been extracted from 15 subbands and one approximation band. Log energy entropy (LEE) feature with conversion as shown below [40]:

$$E_3(s_i) = \log(s_i^2) \tag{2.11}$$

$$E_3(s) = \sum_i \log(s_i^2) \tag{2.12}$$

With the conversion $\log(0) = 0$

Where E is the entropy and $\boldsymbol{E_3(s_i)}$ is known as LEE. s is the signal and $\boldsymbol{s_i}$ is the coefficient of s in orthonormal basis.

2.2.4 Classification Algorithms

2.2.4.1 Decision tree (DT)

Based on the retrieved information, the DT method generates a decision tree with branch and node as a classifier. To reduce the entropy of class labels in the partition, a single feature or many features are considered at each node of the tree [41].

2.2.4.2 Discriminant Analysis (DA)

For data categorization and dimensionality reduction, DA is a widely used approach. When within-class frequencies are not equal and their performances are assessed on randomly generated test information, DA is a simple solution [41].

2.2.4.3 KNN

The KNN method is a classification or regression technique extensively used in machine learning. The idea that physiologically identical samples would have comparable measured values across most of their metabolites is the foundation of KNN. A weighting function is required for varying the distance between the features and gives a better approximation [41].

2.2.4.4 SVM

An SVM discovers a hyperplane that splits attentive and inattentive EEG signal information in its high-dimensional feature spaces. SVM selects the hyperplanes based on the accuracy acquired with the nearest training sample. SVM can classify both nonlinear and linear data. Following that, the SVM tries to build a model and utilizes it to categorize the data [41].

2.2.4.5 Ensemble classifiers

The ensemble classifier is made up of a collection of conventional classification algorithms that are freely mixed to provide results that are superior or equal to the best classification algorithm in the ensemble. Theoretically, the ensemble classifier adapts its performance based on the data being studied, and it eventually achieves the performance of the best-performing individual classifier without knowing it [41].

2.3 Results and Discussion

For the detection of focused, unfocused, and drowsiness mental states, a technique based on FAWT is presented. The 7-channel recorded EEG signal is decomposed into 16 subbands using the FAWT. Initially, 53 features are extracted for each class of EEG signal. The class and subband-wise feature set sizes for focused, unfocused, and drowsiness are 480×7, 480×7, and 1380×7 respectively. In this study, all the subband features are combined for obtaining the classification performance. All 53 features are tested with different machine learning algorithms and the features which are giving comparable better performance are listed in Table 1. From this table, it is observed that LEE is providing better performance as compared to other features. Further, LEE is examined for statistical analysis and different classifiers for obtaining the classification performance.

The statistical analysis of LEE is done by using the Kruskal-Wallis (KW) test. KW test compares independent groups of data in a non-parametric manner. KW test compares the null hypothesis with all the populations having the same distribution functions against the alternative hypothesis such that at least two of the samples differ from one another. KW test results of LEE for different channels and subbands are presented in Table 2.2. In Table 2.2, the LEE feature has considerably obtained lower p-values for all subbands, which shows that the proposed feature has high discriminative power for MI tasks.

Further, the classification of LEE is examined by the DT, DA, SVM, KNN, and ensemble classifiers. The classification performance of these classifiers is evaluated using a 10-fold cross-validation approach. The classification accuracy of weighted KNN and optimizable KNN is significantly greater. Table 2.3 shows the accuracy of all classifier versions for the feature LEE.

The key benefit of utilizing optimizable KNN is that the probability of making an error in a judgment is minimized. There's a potential that noise will damage the samples, but this can be mitigated by utilizing the optimizable KNN, which takes multiple neighbors into account. KNN has a greater chance of producing a better approximation because it considers the likelihood of many synchronous erroneous data points.

S.No	Name of the feature	Accuracy	Classifier
1	Mean Absolute Deviation [43]	87.2%	Weighted KNN
2	Mean Absolute Value [42]	91.3%	Optimizable KNN
3	Average Amplitude Change [42]	90.5%	Optimizable KNN
4	Wavelength [42]	89.4%	Optimizable KNN
5	Negative Entropy [42]	89.2%	Optimizable KNN
6	LEE [40]	93.25%	Optimizable KNN
7	Log Detector [42]	93.0%	Optimizable KNN
8	Modified mean absolute value type 1 [42]	86.7%	Optimizable KNN

Table 2.1: The accuracies achieved for various features.

The minimum classification error (MCE) plot of optimizable KNN for the LEE feature is shown in Fig. 2.3. It can be observed that MCE is decreased with the increase in the iterations. MCE plot shows the estimated and observed MCE with a circle-shaped point indicating the best-point hyper-parameters (HP) and a square-shaped point indicating minimum error HP. The receiver operating characteristics curve (ROC) of optimizable KNN using LEE is shown in Fig. 2.4. ROC is the technique used to check the quality of the feature. The area under the curve (AUC) calculates the quality of the classifier over the threshold values [1,0]. The quality of the feature can be used to determine true positive (TP) and false positive (FP). TP is the ratio of the number of outcomes with predicted and actual class i to the number of outcomes with predicted class i. FP is the ratio of the number of outcomes that are falsely represented as positive to the outcomes of true negative events. The AUC of optimizable KNN with LEE feature is 0.98, which is closer to the ideal value.

	SB1	SB2	SB3	SB4
Channel 1	3.76×10^{-13}	2.11×10^{-09}	5.75×10^{-12}	5.05×10^{-29}
Channel 2	4.66×10^{-13}	1.10×10^{-41}	1.49×10^{-34}	1.57×10^{-14}
Channel 3	9.99×10^{-35}	6.07×10^{-28}	7.42×10^{-11}	1.38×10^{-07}
Channel 4	1.40×10^{-26}	4.30×10^{-13}	1.20×10^{-03}	3.06×10^{-24}
Channel 5	4.83×10^{-35}	8.83×10^{-26}	2.41×10^{-10}	7.06×10^{-26}
Channel 6	1.32×10^{-09}	1.79×10^{-17}	2.70×10^{-15}	8.57×10^{-55}
Channel 7	8.39×10^{-18}	2.59×10^{-21}	8.23×10^{-19}	6.19×10^{-29}
	SB5	SB6	SB7	SB8
Channel 1	1.87×10^{-41}	2.91×10^{-91}	9.86×10^{-82}	4.07×10^{-40}
Channel 2	6.00×10^{-04}	1.40×10^{-05}	6.94×10^{-31}	1.24×10^{-17}
Channel 3	5.60×10^{-05}	1.79×10^{-37}	3.72×10^{-47}	1.95×10^{-21}
Channel 4	7.91×10^{-40}	8.98×10^{-95}	4.51×10^{-88}	5.22×10^{-43}
Channel 5	2.10×10^{-33}	4.45×10^{-88}	1.83×10^{-97}	6.18×10^{-45}
Channel 6	8.38×10^{-78}	2.45×10^{-110}	1.51×10^{-133}	4.69×10^{-75}
Channel 7	3.34×10^{-49}	8.09×10^{-104}	1.53×10^{-146}	1.33×10^{-99}
	SB9	SB10	SB11	SB12
Channel 1	4.76×10^{-11}	4.56×10^{-12}	1.39×10^{-13}	1.56×10^{-20}
Channel 2	3.64×10^{-28}	2.22×10^{-32}	3.10×10^{-41}	2.93×10^{-51}
Channel 3	1.81×10^{-66}	3.58×10^{-96}	1.38×10^{-119}	3.84×10^{-110}
Channel 4	2.97×10^{-89}	1.62×10^{-156}	1.97×10^{-184}	1.59×10^{-176}
Channel 5	1.52×10^{-68}	4.01×10^{-111}	1.18×10^{-127}	1.15×10^{-122}
Channel 6	1.73×10^{-22}	7.18×10^{-15}	1.98×10^{-10}	1.75×10^{-18}
Channel 7	3.00×10^{-30}	3.30×10^{-17}	3.56×10^{-08}	5.21×10^{-05}
	SB13	SB14	SB15	SB16
Channel 1	3.40×10^{-10}	8.77×10^{-07}	9.57×10^{-06}	1.73×10^{-05}
Channel 2	5.65×10^{-51}	3.11×10^{-27}	7.59×10^{-29}	1.55×10^{-24}
Channel 3	4.69×10^{-108}	2.79×10^{-86}	1.96×10^{-72}	4.53×10^{-09}
Channel 4	2.98×10^{-150}	5.94×10^{-110}	1.03×10^{-69}	1.16×10^{-15}
Channel 5	2.00×10^{-94}	9.17×10^{-77}	9.74×10^{-56}	2.71×10^{-02}
Channel 6	1.03×10^{-07}	2.43×10^{-05}	2.77×10^{-08}	1.57×10^{-02}
Channel 7	4.00×10^{-04}	3.04×10^{-02}	5.90×10^{-03}	3.18×10^{-02}

Table 2.2: The KW test values of the feature LEE.

Classifiers	*Classifier variants*	*Accuracy*
	Fine tree	74.2
	Medium tree	68.8
DT	Coarse tree	65.2
	Optimizable tree	75.7
	Linear discriminant	76.6
DA	Quadratic discriminant	85.1
	Optimizable discriminant	85.1
	Linear SVM	75.4
	Quadratic SVM	89.1
	Cubic SVM	91.0
SVM	Fine Gaussian SVM	61.1
	Medium Gaussian SVM	88.2
	Coarse SVM	68.5
	Optimizable SVM	90.3
	Fine KNN	91.9
	Medium KNN	91.2
	Coarse KNN	71.7
k-NN	Cosine KNN	89.8
	Cubic KNN	90.0
	Weighted KNN	92.2
	Optimizable KNN	93.0
	Boosted trees	77.5
	Bagged trees	85.8
	Subspace discriminant	75.6
Ensemble classifiers	Subspace KNN	89.3
	RUSBoosted trees	72.9
	Optimizable ensemble	88.0

Table 2.3: The accuracies of various classifiers using the feature LEE.

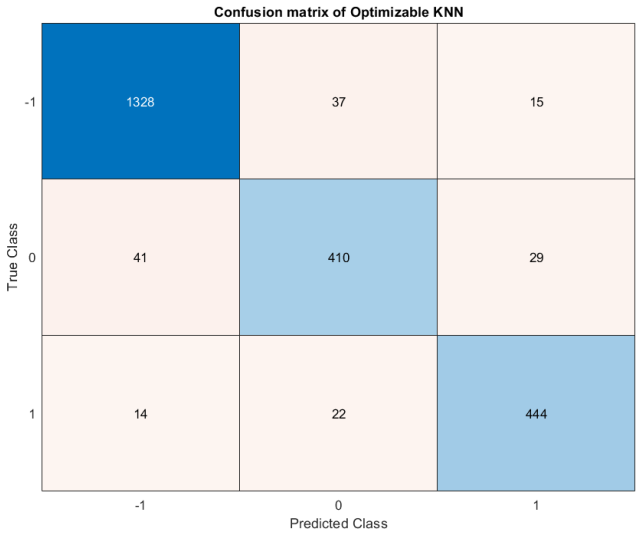

Fig. 2.2. The confusion matrix of optimizable KNN using LEE feature.

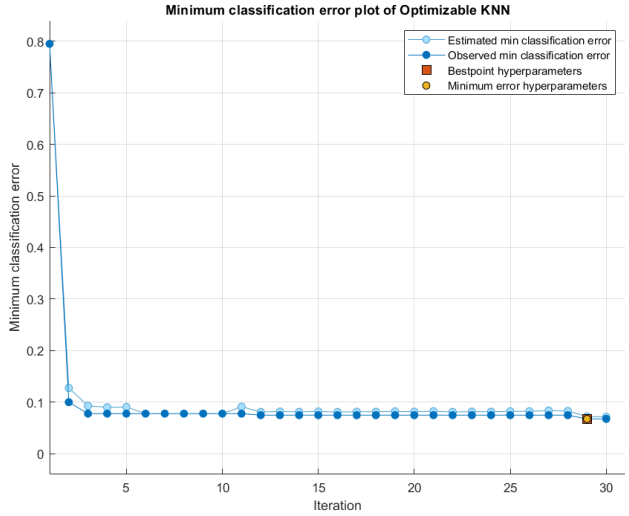

Fig. 2.3. The MCE plot of optimizable KNN using LEE feature.

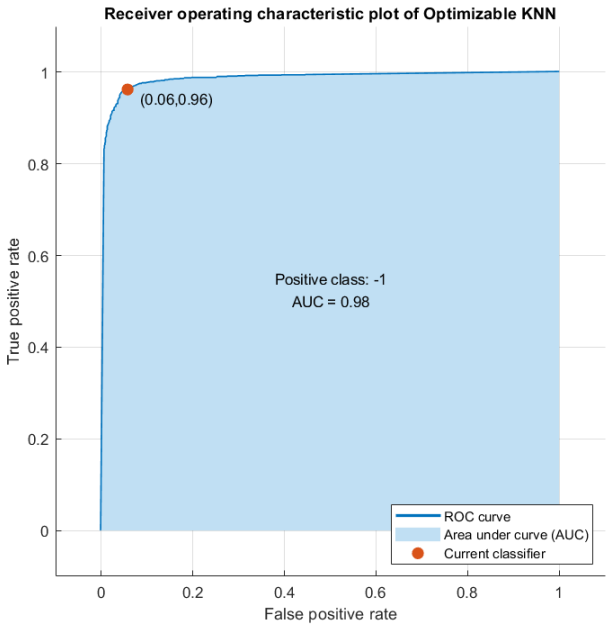

Fig. 2.4. The ROC of optimizable KNN using LEE feature.

The performance measures for the proposed feature are presented in Table 2.4. Table 2.4 explains that the suggested method's misclassification rate of 6.75% is much lower, indicating that both classes of EEG signals are correctly classified. The sensitivity (SEN) of 91.38% and specificity (SPE) of 96.24% are quite close to the optimum values of sensitivity and specificity. Precision and recall are defined by the F1-score composite. The F1 score for the suggested technique is 0.9142, which is closer to its maximum value. The classification performance was evaluated using Matthew's correlation coefficient (MCC). The MCC value achieved by the proposed method is 87.70%, which is closer to the ideal value.

The confusion matrix of optimizable KNN using the LEE feature is shown in Fig 2.2. The predicted class is represented by the rows of the confusion matrix, while the target class is represented by the columns. Perfectly classified elements are represented in diagonal elements, and the remaining elements are incorrectly classified.

Performance measure (Ideal value)	Classification performance
AC (100%)	93.25%
Error (0%)	6.75%
Sen (100%)	91.38%
Spe (100%)	96.24%
Precision (100%)	91.48%
F_1 (1)	0.9142
M_{CC} (100%)	87.70%
Kappa (1)	0.8481

Table 2.4: The suggested classification model's performance metrices.

The utility of the suggested strategy is now demonstrated by a comparison of various studies conducted for the MI tasks classification is presented in Table 2.5. The techniques are contrasted in terms of the classifier, and accuracy that have been provided. Li et al used the FIR filtering approach with KNN to classify five mental states [29]. The fast Fourier transform (FFT) with an SVM-based approach is used by Myrden et al, Liu et al and Wang et al with the accuracy of 71.6%, 76.82%, and 84.6% respectively. The mental states predicted by Myrden et al, Liu et al and Wang et al are 3 states, 2 states, 2 states [30, 32, 34]. Similarly, Ke et al used wavelet transform with SVM have achieved an accuracy of 76.19% with 3 mental states predicted [31]. Cigdem et al have used the same dataset used in this work with STFT with the SVM approach and achieved an accuracy of 91.72% [35]. Smith et al using the same dataset have achieved an accuracy of 91.77% with RDWT and BT [36]. Sachin et al used EMD with the MS-LS-SVM approach and achieved an accuracy of 90.63% [37]. The performance metrics SEN, SPE, Accuracy, and MCC obtained by the suggested technique are 91.20%, 96.21%, 93.16%, and 87.51%, respectively.

Authors	Dataset used	Proposed method	Classification algorithm	Mental states predicted	Classification performance (Accuracy achieved)
Li et al [29]	EEG	FIR filtering	KNN	5 states (happy, surprise, fear, disgust, and neutral)	57.0%
Myrden and Chau et al [30]	EEG	FFT	SVM	3 states (fatigue, frustration, attention)	71.6%
Ke et al [31]	EEG	WT	SVM	3 states (attention, no attention, reset)	76.19%
Liu et al [32]	EEG	FFT	SVM	2 states (attentive and in-attentive)	76.82%
Djamal et al [33]	EEG	Wavelet Filtering	SVM	3 states (happy, relax, sad)	77.0%
Wang et al [34]	EEG	FFT	SVM	2 states (driving and math task)	84.6%
Sachin et al [37]	EEG	EMD	MS-LS-SVM	4 states (happy,	90.63%

				fear, sad and relax)	
Çiğdem et al [35]	EEG	STFT	SVM	3 states (focused, unfocused and drowsing)	91.72%
Smith et al [36]	EEG	RDWT	BT	3 states (focused, unfocused and drowsing)	91.77%
Proposed method	EEG	FAWT	KNN	3 states (focused, unfocused and drowsiness)	93.25%

Table 2.5: The suggested method's performance summary in comparison to existing mental states identification.

2.4 Summary

In this study, the FAWT technique-based features are introduced for the classification of focused, unfocused, drowsiness mental states EEG signals. The LEE feature is explored for analyzing FAWT-provided sub-bands. The KW test ensures the statistical significance of LEE. The LEE is computed from all sub-bands are tested on several machine learning techniques. The optimizable KNN provides the best classification as follows: accuracy is 93.25%, sensitivity is 91.38%, specificity is 96.24%, precision is 91.48%, the F1-score is 91.42%, and kappa value is 0.8481. The results are compared with the existing works and the proposed work is obtained best classification performance. The proposed approach can be explored in the clinical based applications for detecting different neurological disorders and classification of other bio-medical signals.

CHAPTER 3
Normal and Alcohol EEG Signals Classification Using Singular Spectrum Analysis

3.1 Introduction

Consumption of alcohol has far reached socio-cultural and economic consequences for the drinkers. An increase in traffic accidents, machine-related mishaps, and violence are some results of drinking. Regular intake of alcohol damages the organs and DNA of human beings. Drinking leads to the third position in diseases. Alcoholism-related genetic diseases include weaker and less organized theta rhythms [44]. Drinking is the third major cause of disease as per the world health organization [45]. Furthermore, alcoholism increases as per disability-adjusted life-years (DALY) which estimates that 5.1% of global diseases are related to alcohol consumption [46]. Furthermore, the rising incidence of malignancies linked to alcohol adds to the seriousness of the situation [47]. These negative consequences highlight the importance of enhanced researches aiming at price efficient and early alcohol misuse monitoring and diagnosis [48]. The non-invasive nature of electroencephalogram (EEG)-based techniques makes it more viable for real-time diagnosis of alcoholics [49].

3.2 Literature Survey

Several studies are conducted for the identification of alcohol EEG data. A variational mode and empirical mode decompositions (EMD) with least Square Support Vector Machine (LS-SVM), and K-Nearest Neighbor (KNN) algorithms are employed for the identification of alcohol EEG signals [50]. A wavelet filter bank-based approach is suggested for the identification of the alcohol EEG signals [51]. Kolmogorov-Smirnov test-based features are explored with Adaboost k-means algorithms for identifying alcohol EEG signals [52]. The EMD based feature extraction with ensemble subspace KNN based classification is explored to identify alcohol EEG signals [53]. A test to check the ability of parametric spectrum and coherence estimators and phase synchrony processor, which identifies the variations in the scalp while eyes remained open in both alcohol and normal EEG data is explored [54]. A fast Fourier transform and autoregression modeling are explored for the identification of alcohol EEG signals with discriminant analysis (DA) [55]. A tunable-Q wavelet transform (TQWT) with ensemble classifiers are explored for the identification of apnea events [56]. For the

automatic identification of alcoholics, the nonlinear features of computer-aided diagnostics are examined with SVM [57]. Higher-order spectrum cumulants and other non-linear features are extracted to assess alcohol-related alterations in EEG data, various machine learning algorithms are employed to classify alcohol EEG data [58]. The classification of alcohol EEG is explored by wavelet packet decomposition with KNN is presented [59]. The automatic identification of alcohol EEG signals is done by using a time-frequency image-based technique is suggested [60]. The diagnosis of alcoholics is explored by the TQWT with SVM [61]. The correlation analysis is adopted for the statistical analysis and KNN is explored to identify alcohol EEG data [62]. EMD with extreme machine learning and SVM algorithms are explored for the analysis of alcohol EEG signals using EEG rhythms is proposed [63]. The identification of alcohol EEG data is explored by using wavelet transform with Extreme learning machine (ELM) [64]. The power spectral density (PSD) is explored to identify the changes in alcohol EEG signals is presented [65]. Principle component analysis and singular value decomposition-based extracted features are employed to classify the alcohol EEG data with KNN is explored [66]. PSD of the haar mother wavelet-based features is explored to classify the alcohol EEG data with SVM [67]. The automated identification of alcohol EEG signals is explored using a dual-tree complex WT and SVM classifier [68].

This work suggested singular spectrum analysis (SSA) and an optimizable classifier-based algorithm to classify the alcohol EEG data. SSA-based features were extracted and further driven to multiple classifiers for the classification.

3.3 Methodology

3.3.1 Dataset

The validation of the suggested methodology is done by using the dataset which contains EEG data of alcoholic and normal person respectively. The dataset can be provided online [69]. The signals are acquired using 64 electrodes which has a sampling frequency of 256 Hz. A total 120 EEG signals are used with 2048 sample lengths are considered in this work to distinguish normal and alcohol people. Fig. 3.1 shows the block diagram of the proposed work.

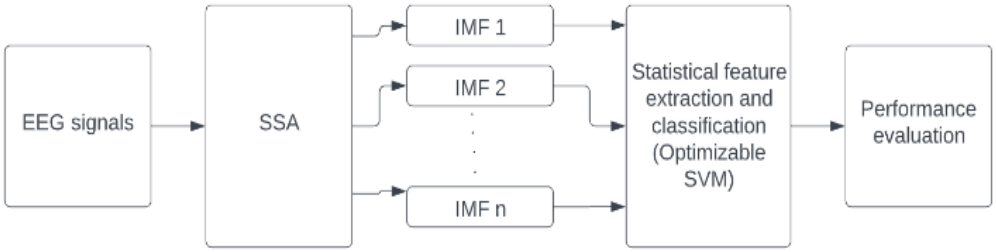

Fig. 3.1. Block diagram of proposed methodology.

3.3.2 Singular Spectrum Analysis

The SSA is a non-parametric technique that is frequently accessed to analyze meteorological and geophysical data series [70]. SSA is made up of two steps: embedding and reconstruction. During the embedding process, the EEG data vector S is mapped with a multivariate data matrix with arranging the *K* number of delayed vectors with a size *D*, which in-turn yields to a trajectory matrix (TM) *T* of size *A*×*B* is given as [70].

$$T_{A\times B} = \begin{bmatrix} t(1) & t(2) & \dots & \dots & t(K) \\ t(2) & t(3) & \dots & \dots & t(K+1) \\ \vdots & \vdots & \dots & \dots & \vdots \\ t(D) & t(D+1) & \dots & \dots & t(N) \end{bmatrix} \quad (3.1)$$

Here K=N-D+1 and D stands for window length and can be defined for D > $\frac{fs}{f}$, where f_s stands for sampling frequency and frequency of the signal is represented by f. The TM is further decomposed into M number of TM, T_1, T_2, T_3, ..., T_M, in the last stage of SSA.

3.3.3 Feature Extraction and Classification

This work uses IQR and wavelength (WAVELEN) as features. The difference of third quartile to the first quartile is IQR [71]. IQR can be calculated by obtaining the center point of both the upper and lower half of the data. Wavelength is defined as the EEG waveform's cumulative length across a time segment [72].

In this work SVM is explored to solve two class classification problem. The goal of the SVM algorithm is to find the Optimal Separating hyperplane, which separates the samples while also maximizing the distance between the two classes [73].

3.4 Results and discussion

For the identification of alcohol and normal EEG data, a technique based on SSA is presented. The data comprises 53 features with two classes (i.e., normal and alcohol). Each class has 16 subbands (SB) with a feature set of *1×120* for both alcohol and normal respectively. The Kruskal-Wallis (KW) test compares three or more independent groups of data in a non-parametric manner. The KW test is used to perform a discriminative analysis of derived features. The features having smaller probabilistic ($p<0.05$) values are considered for the classification because of the high discriminative power for EEG signals. KW test results are shown in Table 3.1. The KW test plots of IQR are shown in Fig. 3.2.1 to Fig. 3.2.16. The KW plots of WAVELEN are shown from Fig. 3.3.1 to Fig. 3.3.16. The SBs 2, 4, 5, 6, 7, 8, 9, 10, 11, 12, 16 has lower *p* value as shown in Table 3.1 are considered for the classification. A 10-folds cross-validation method is used at the classifier stage. The features are tested with all the variants of the SVM algorithm. Table 3.2 presents the achieved accuracy of the proposed features using the SVM classifier. Optimizable SVM gives a better accuracy of 94.2% when compared to all other variants of SVM.

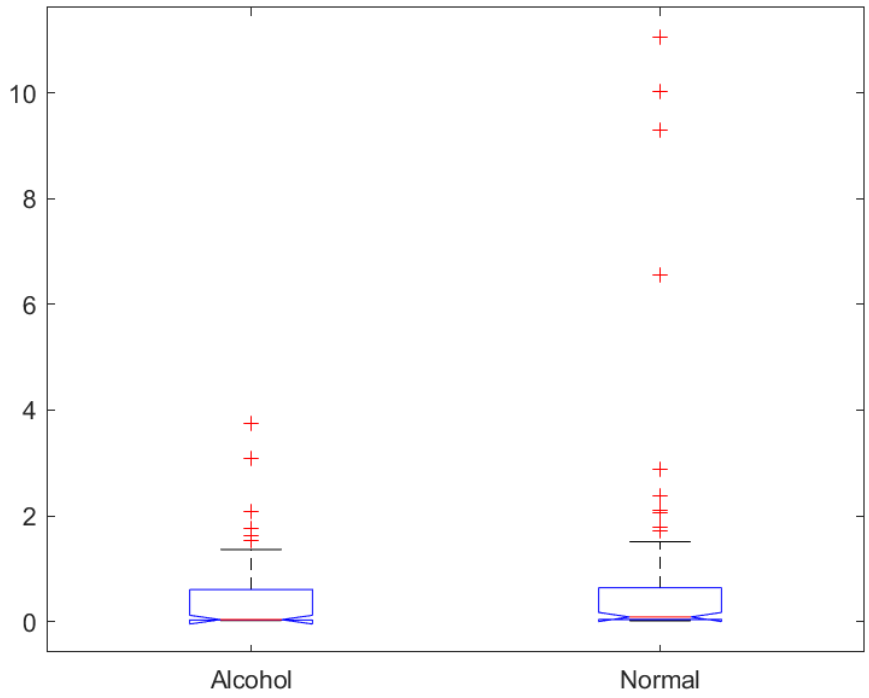

Fig. 3.2.1. IQR SB1 KW test plot.

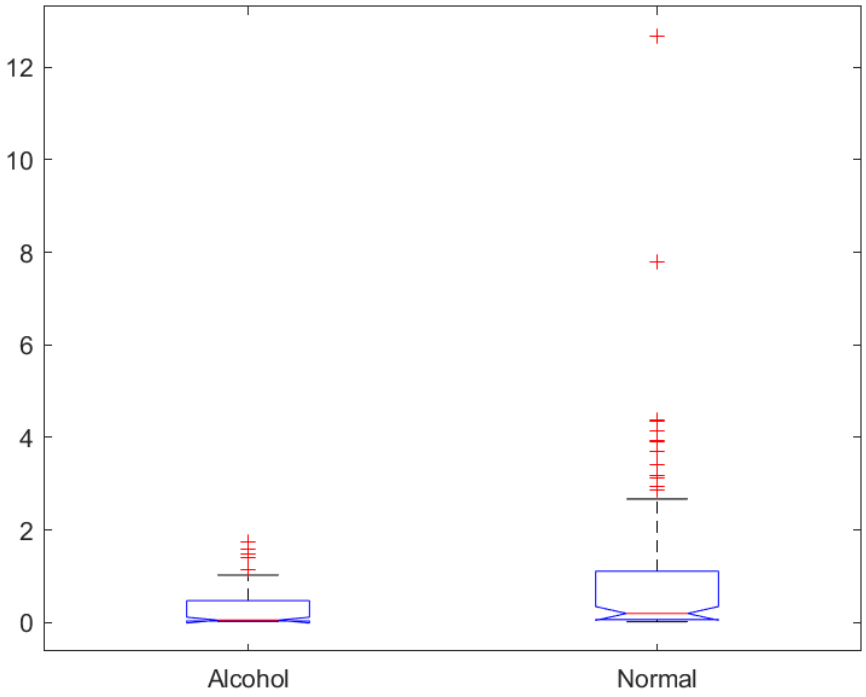

Fig. 3.2.3. IQR SB2 KW test plot.

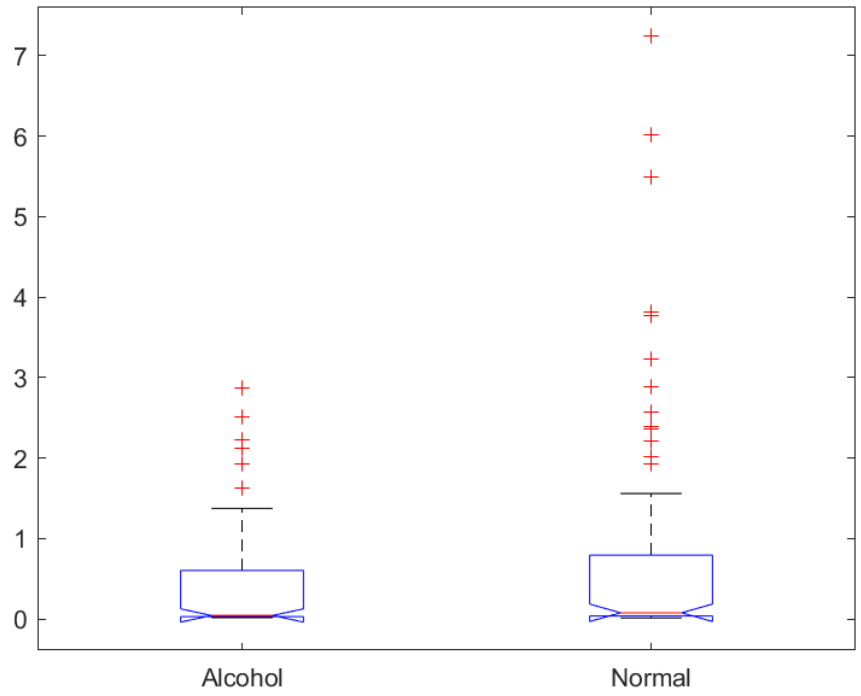

Fig. 3.2.3. IQR SB3 KW test plot.

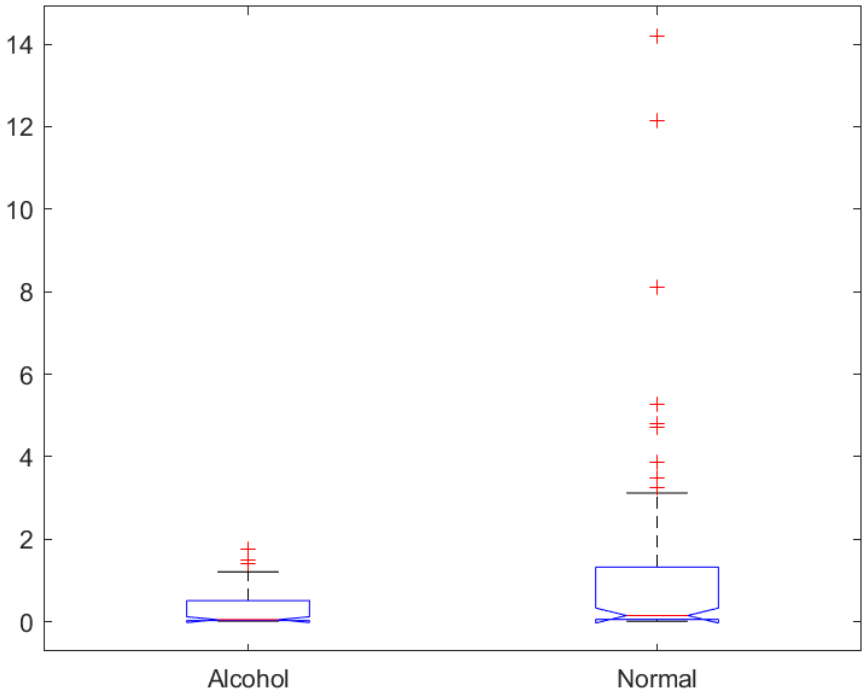

Fig. 3.2.4. IQR SB4 KW test plot.

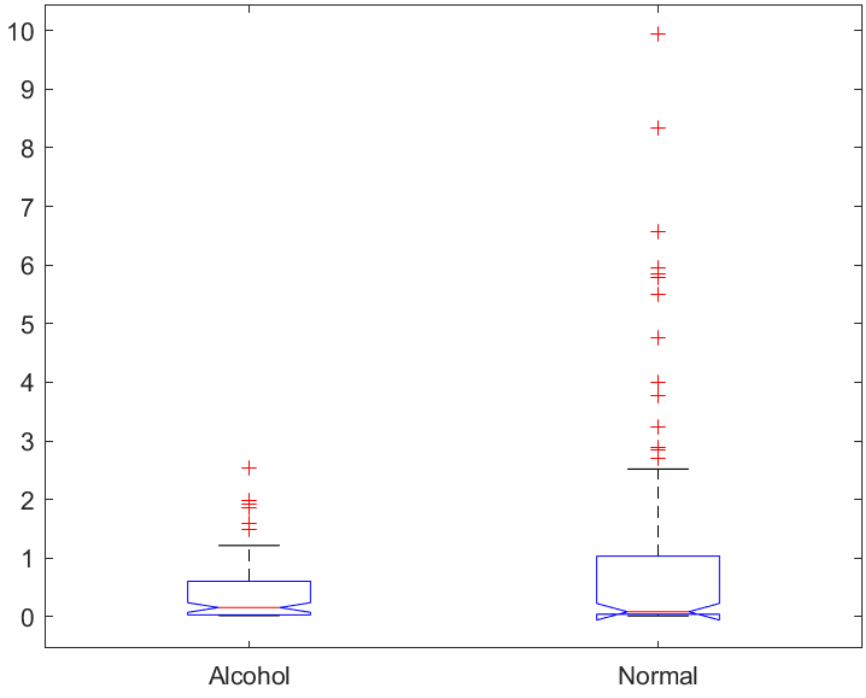

Fig. 3.2.5. IQR SB5 KW test plot.

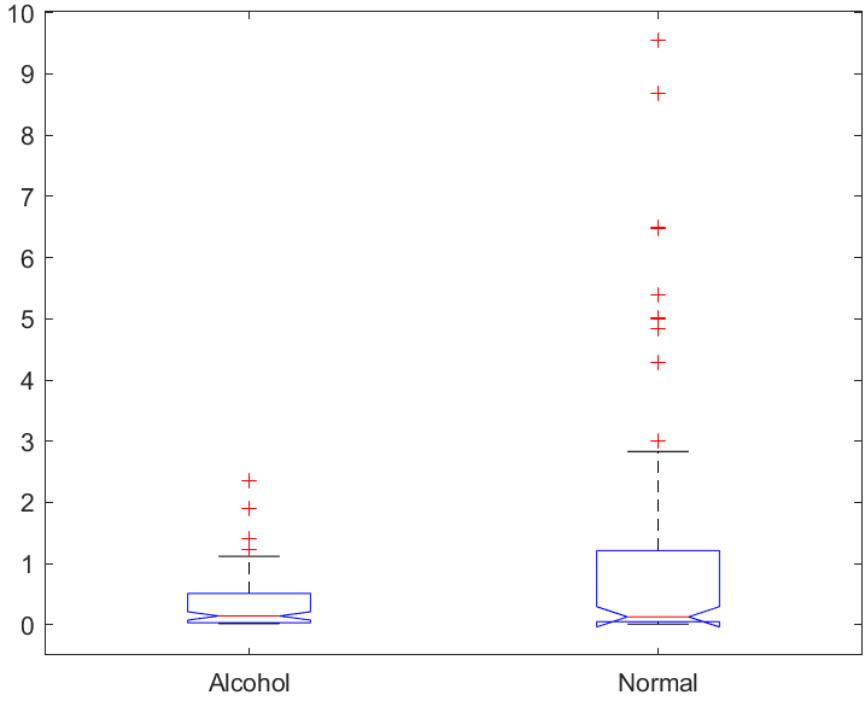

Fig. 3.2.6. IQR SB6 KW test plot.

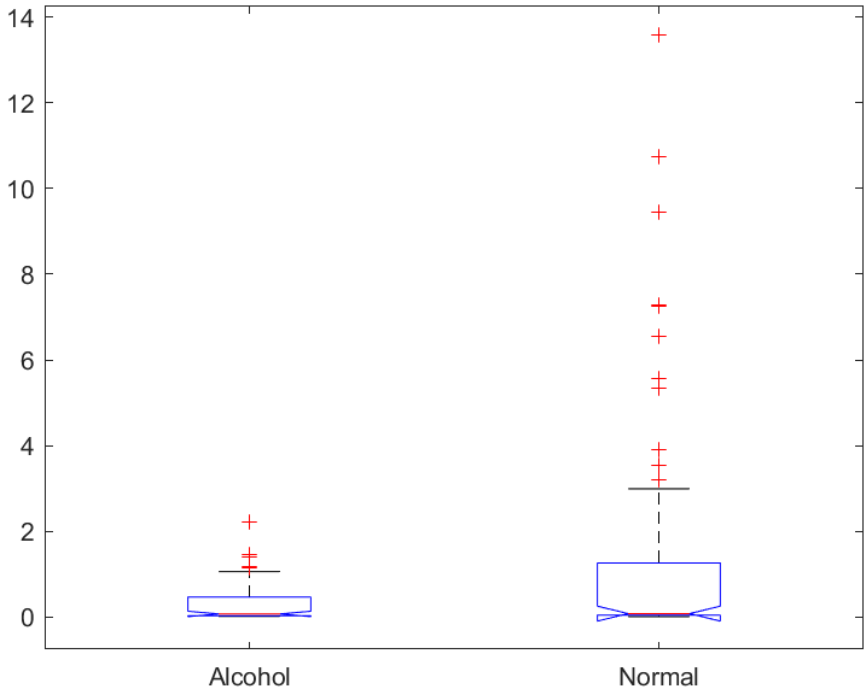

Fig. 3.2.7. IQR SB7 KW test plot.

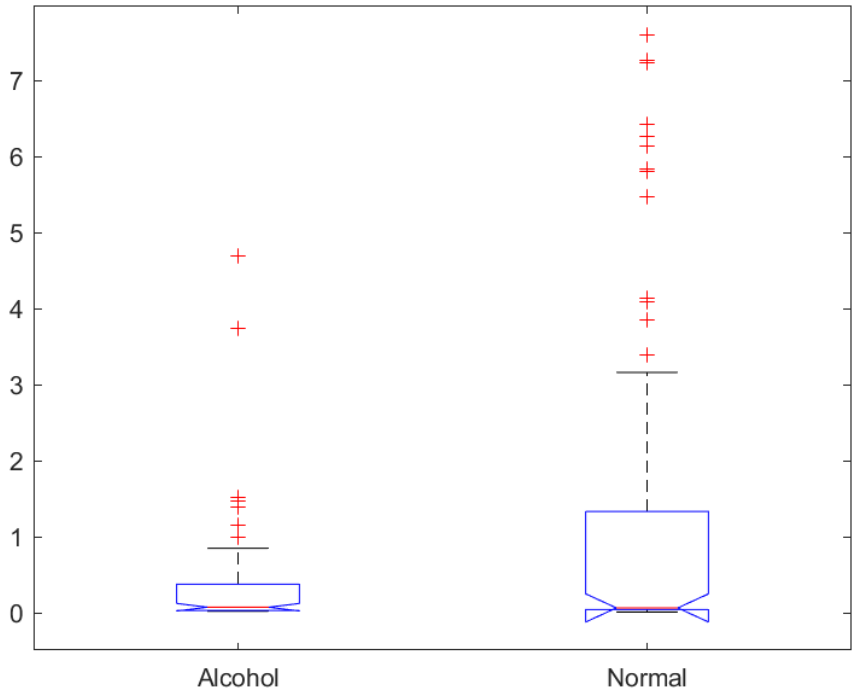

Fig. 3.2.8. IQR SB8 KW test plot.

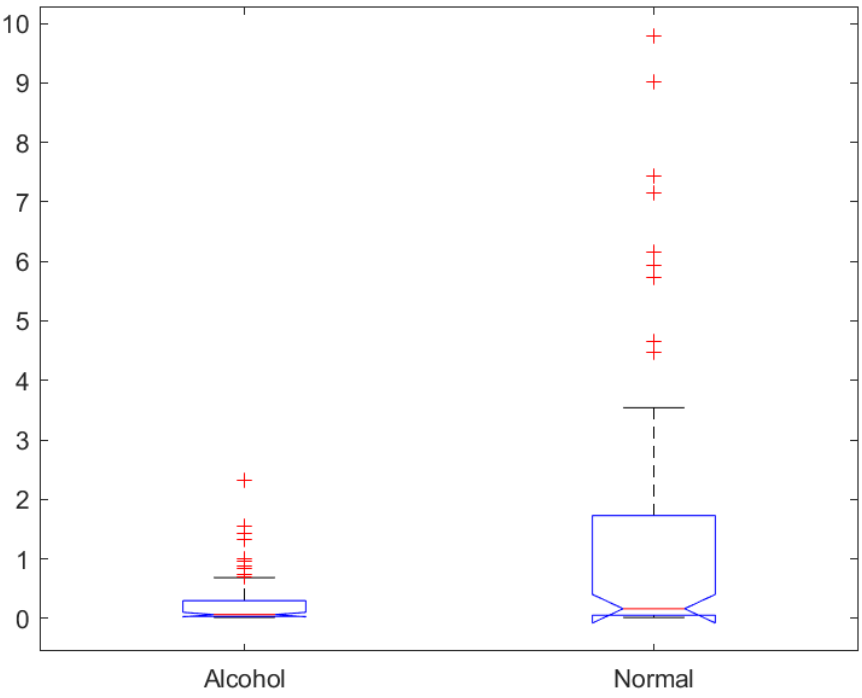

Fig. 3.2.9. IQR SB9 KW test plot.

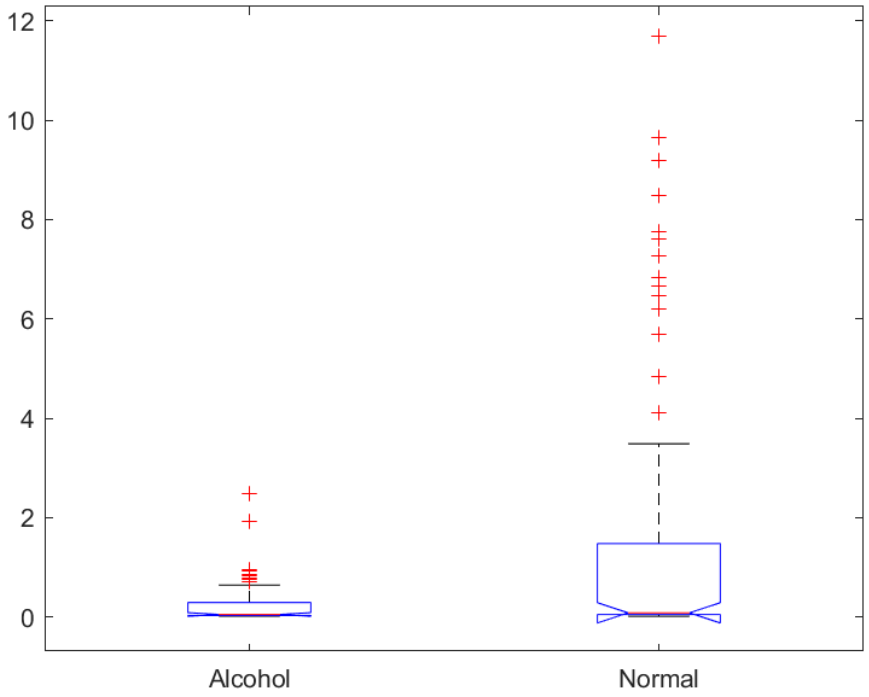

Fig. 3.2.10. IQR SB10 KW test plot.

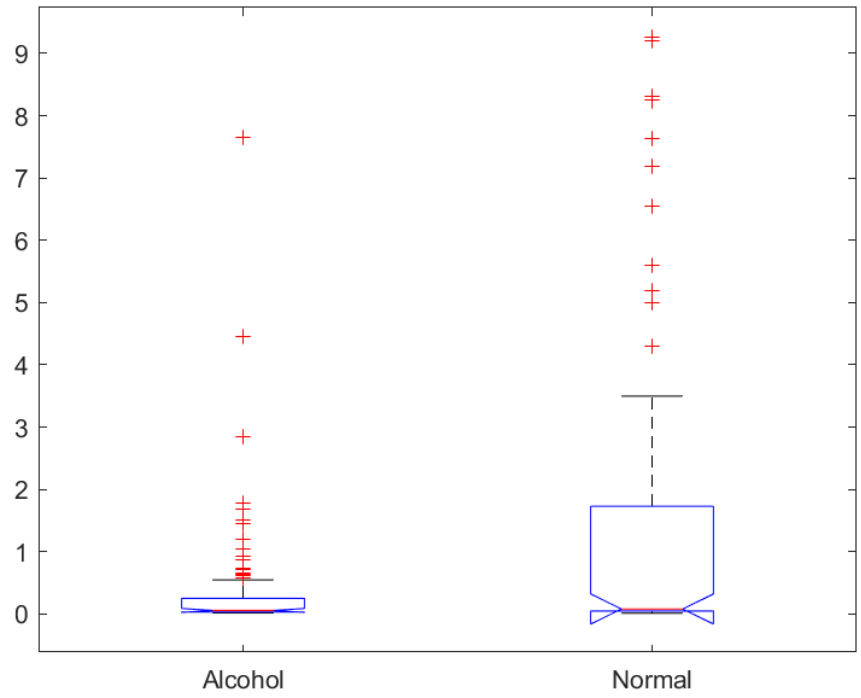

Fig. 3.2.11. IQR SB11 KW test plot.

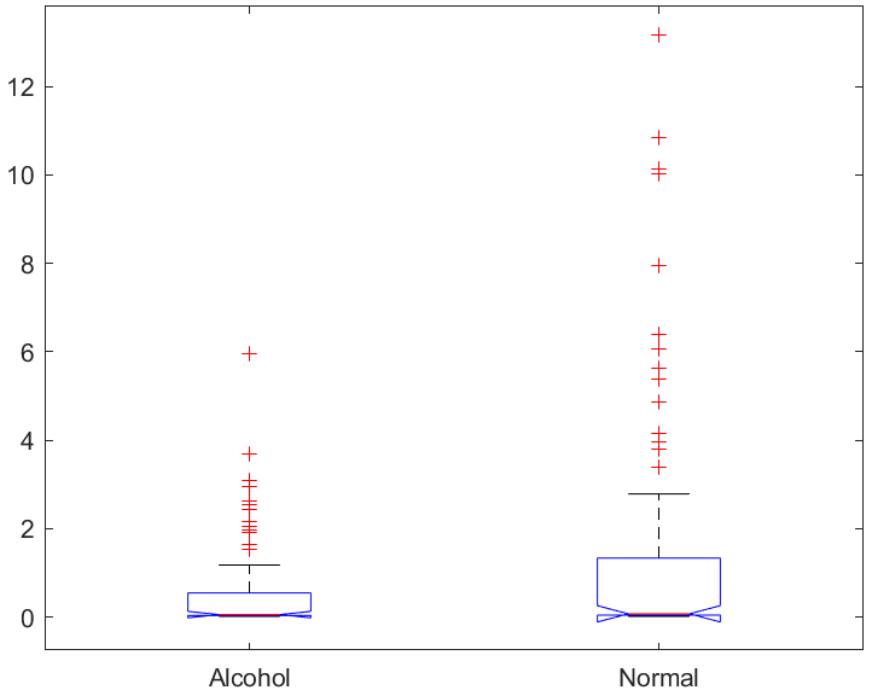

Fig. 3.2.12. IQR SB12 KW test plot.

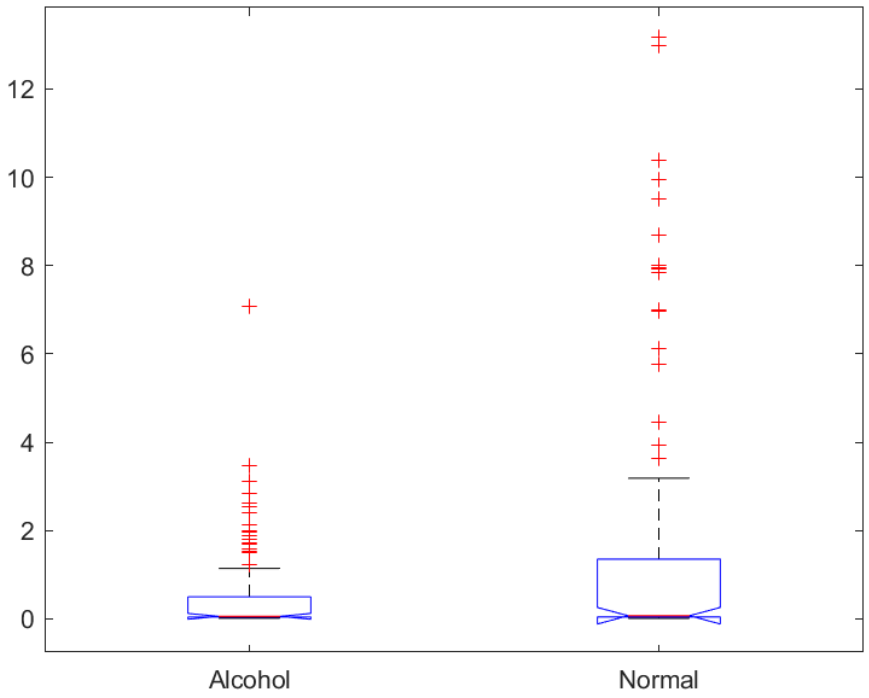

Fig. 3.2.13. IQR SB13 KW test plot.

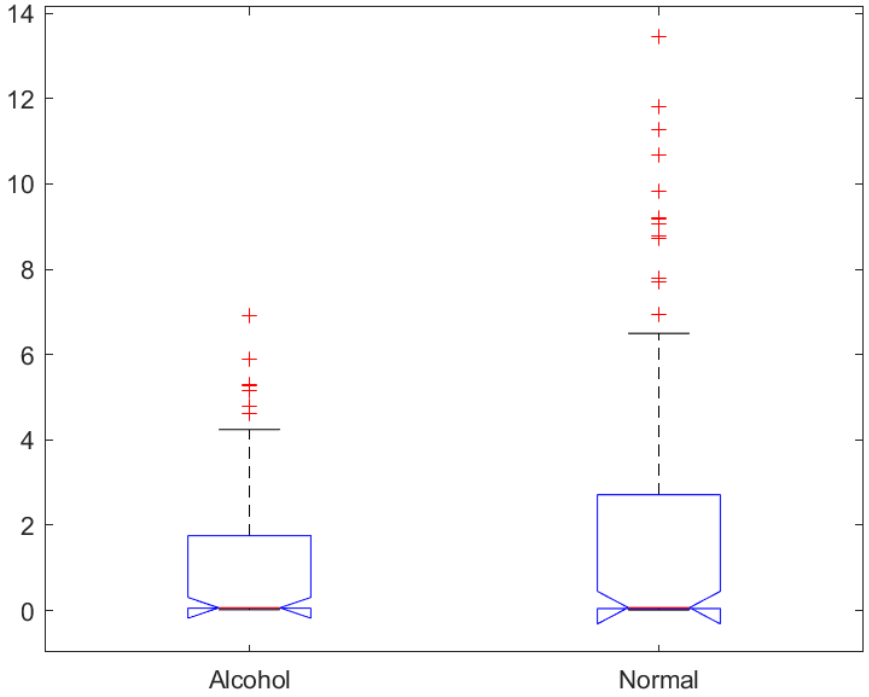

Fig. 3.2.14. IQR SB14 KW test plot.

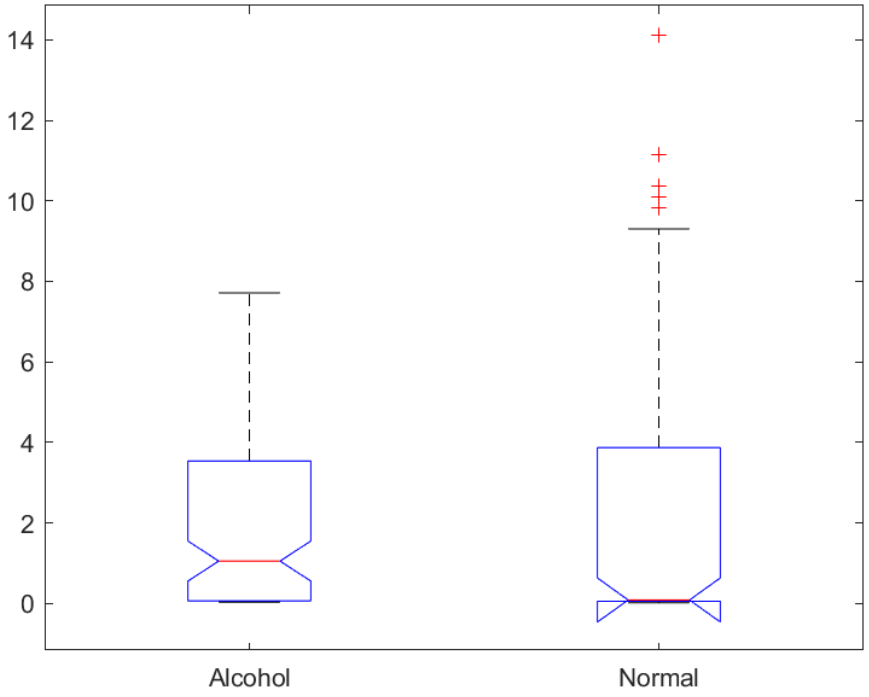

Fig. 3.2.15. IQR SB15 KW test plot.

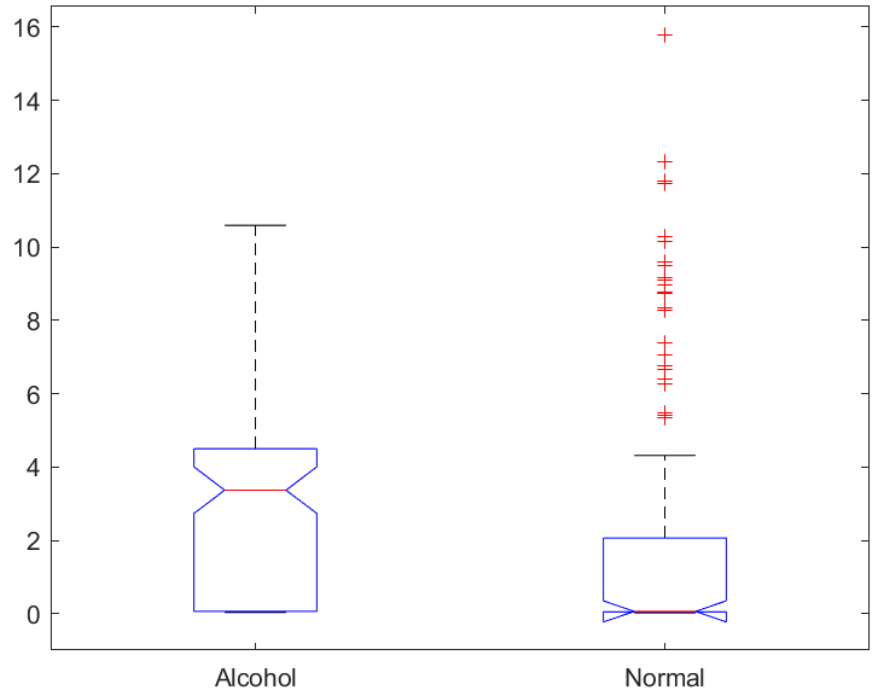

Fig. 3.2.16. IQR SB16 KW test plot.

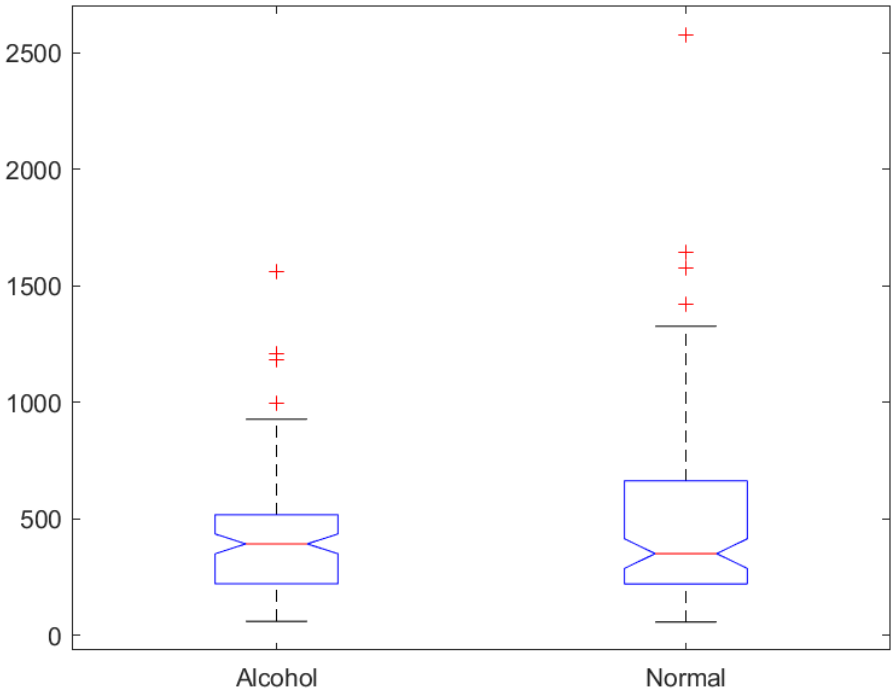

Fig. 3.3.1. WAVELEN SB1 KW test plot.

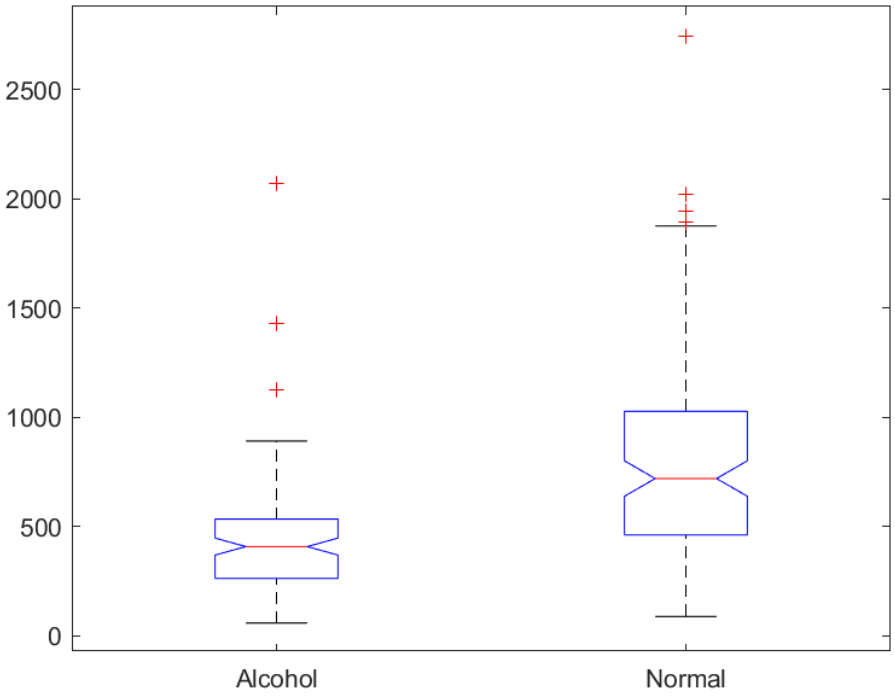

Fig. 3.3.2. WAVELEN SB2 KW test plot.

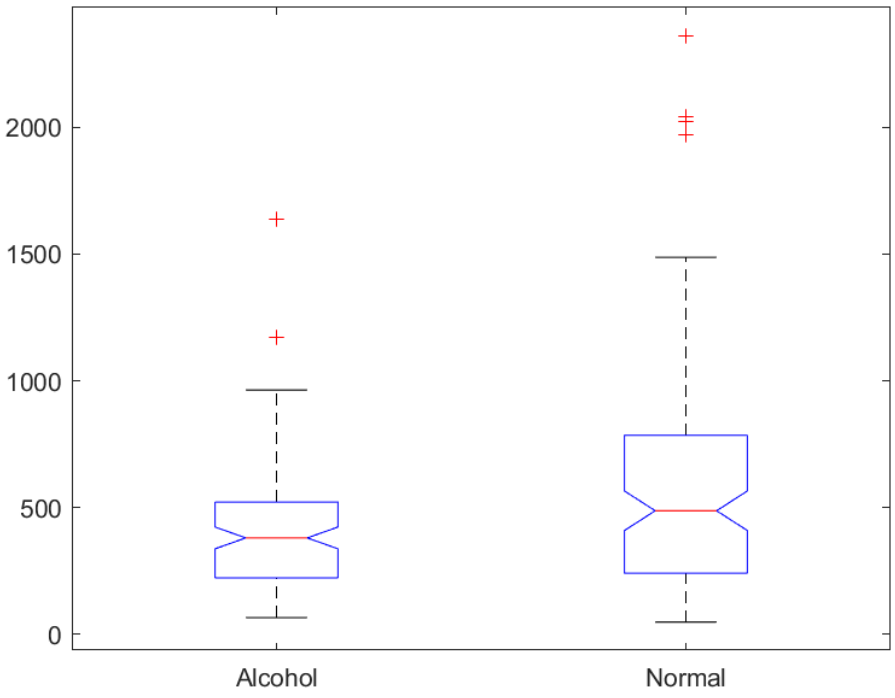

Fig. 3.3.3. WAVELEN SB3 KW test plot.

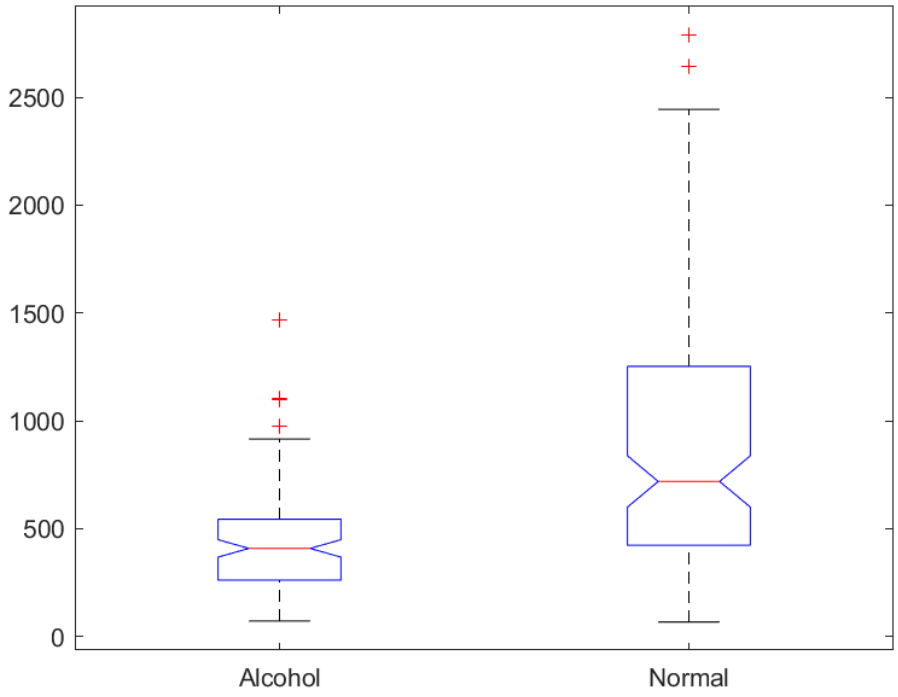

Fig. 3.3.4. WAVELEN SB4 KW test plot.

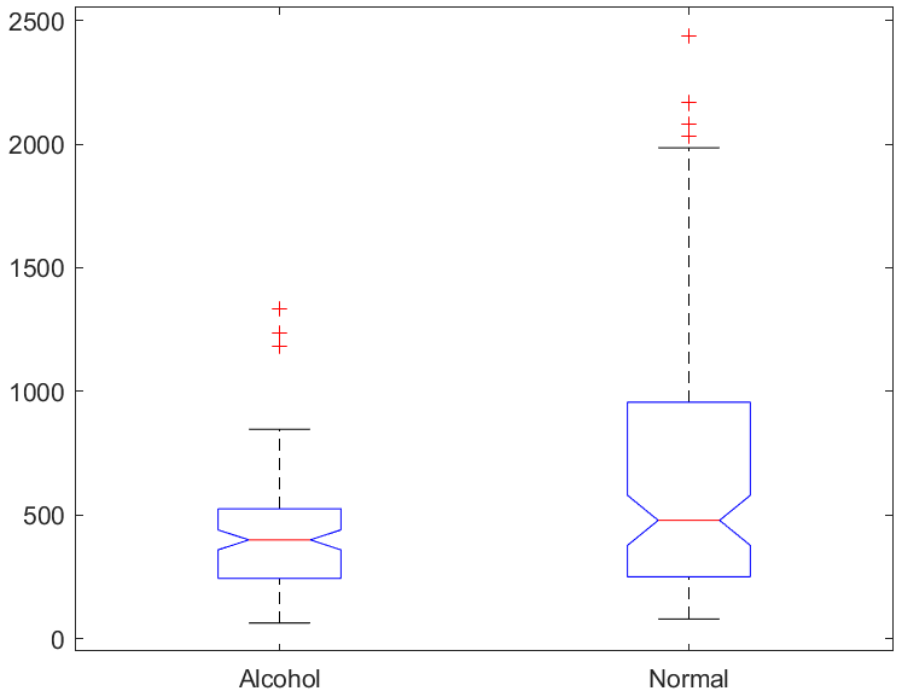

Fig. 3.3.5. WAVELEN SB5 KW test plot.

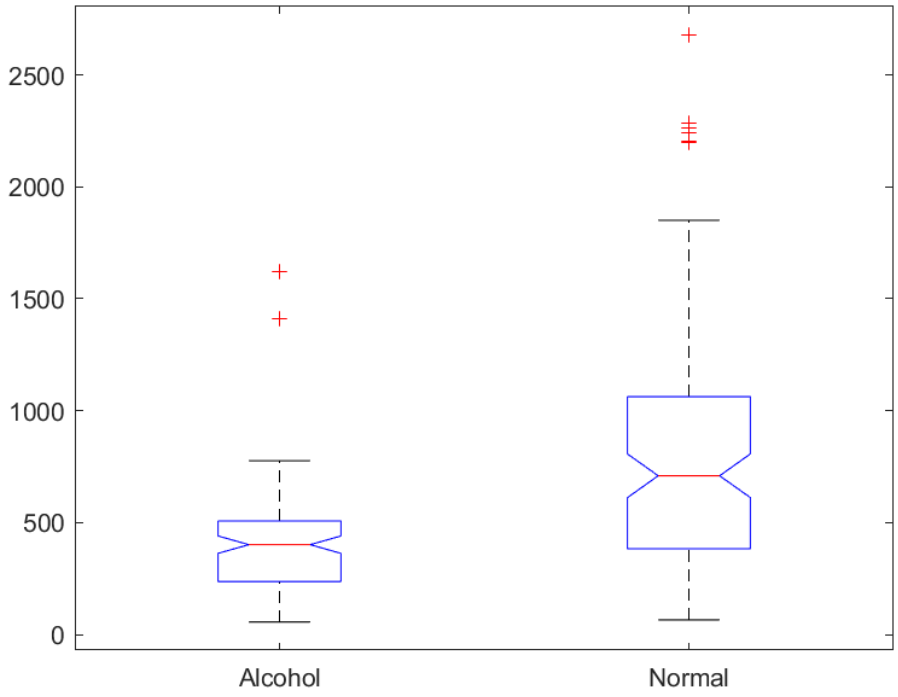

Fig. 3.3.6. WAVELEN SB6 KW test plot.

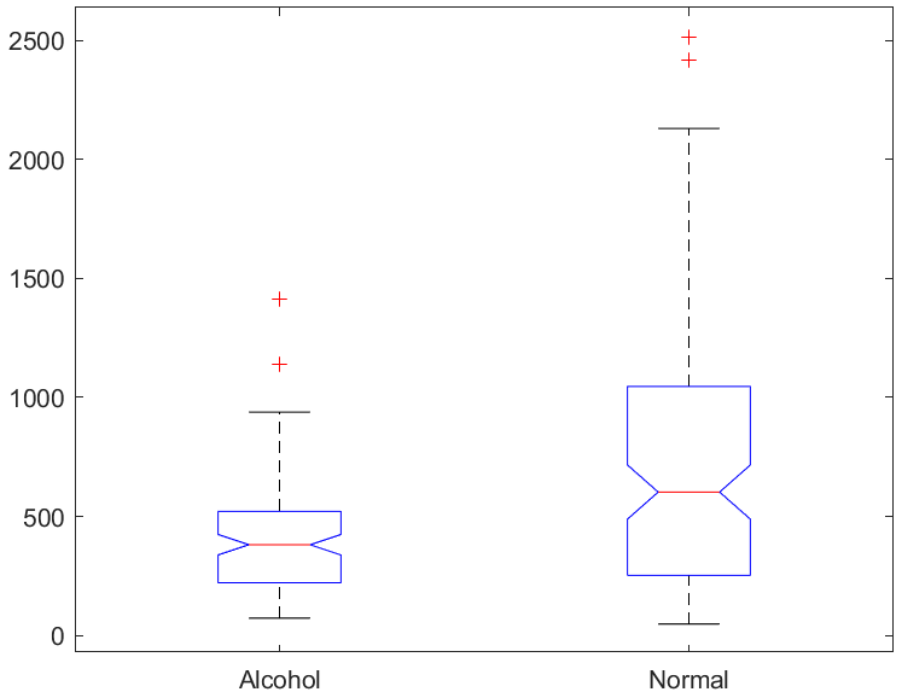

Fig. 3.3.7. WAVELEN SB7 KW test plot.

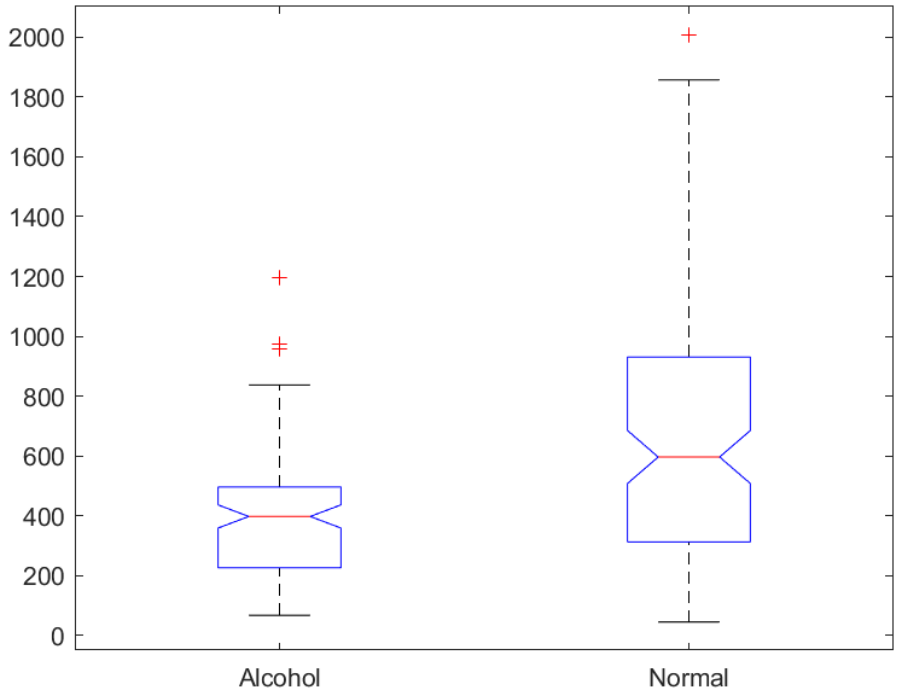

Fig. 3.3.8. WAVELEN SB8 KW test plot.

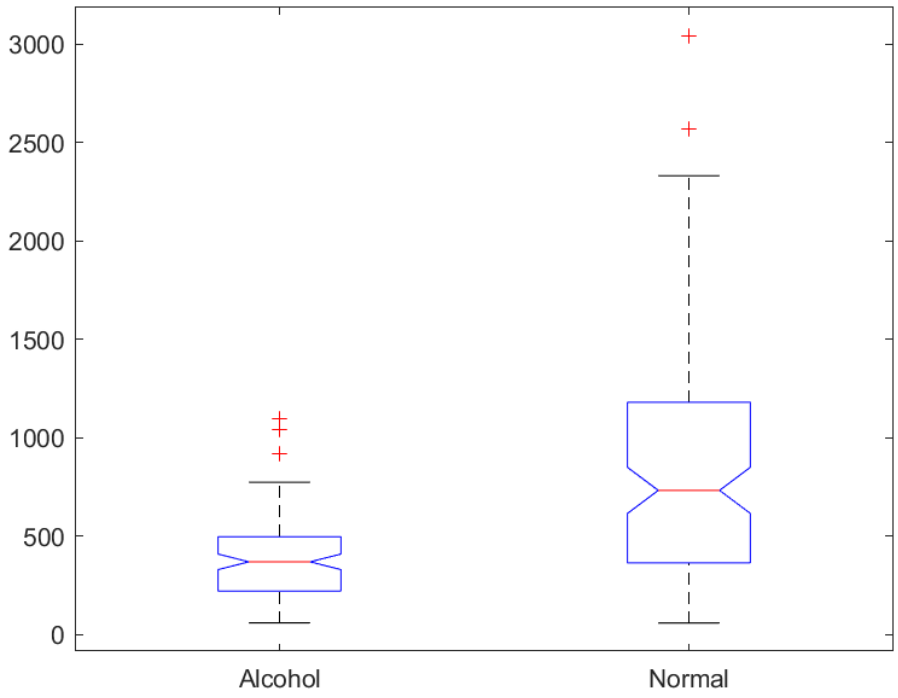

Fig. 3.3.9. WAVELEN SB9 KW test plot.

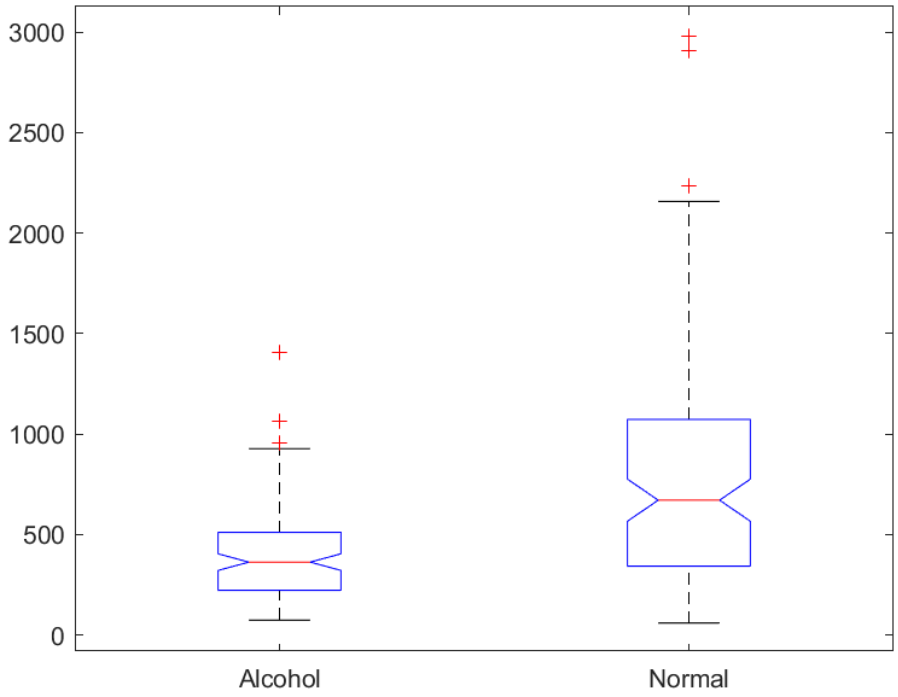

Fig. 3.3.10. WAVELEN SB10 KW test plot.

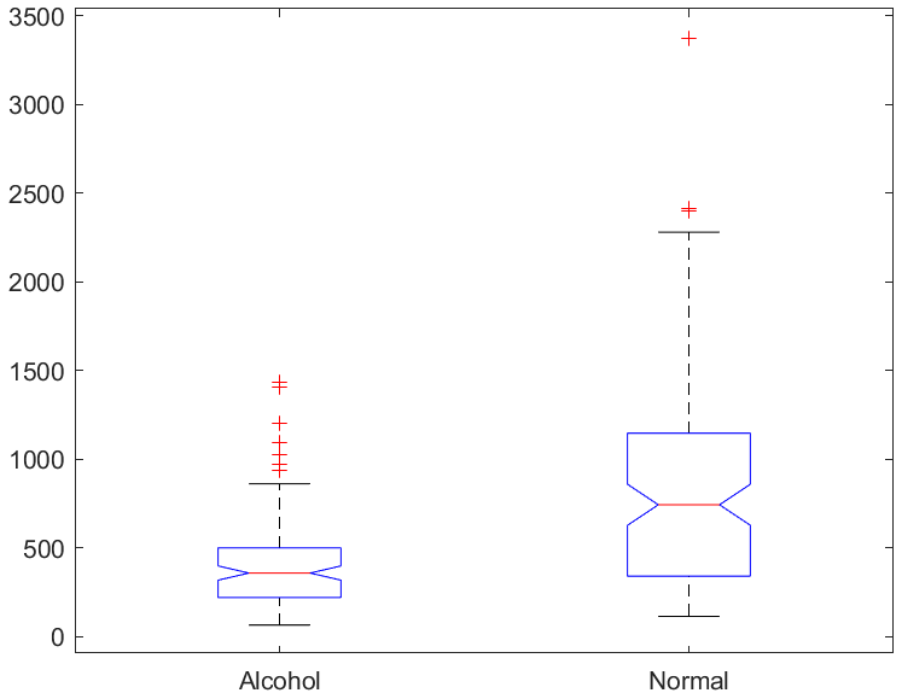

Fig. 3.3.11. WAVELEN SB11 KW test plot.

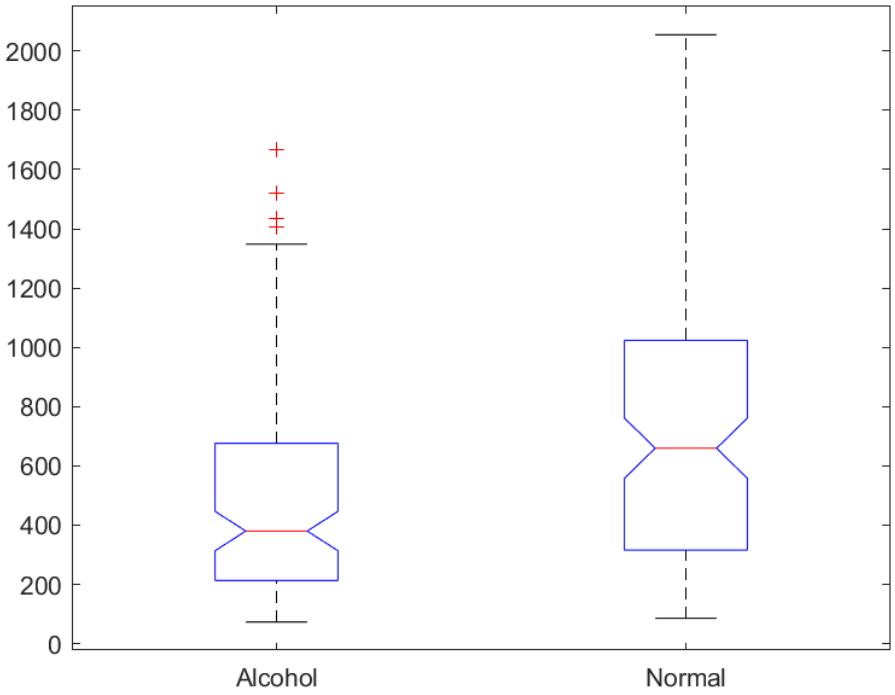

Fig. 3.3.12. WAVELEN SB12 KW test plot.

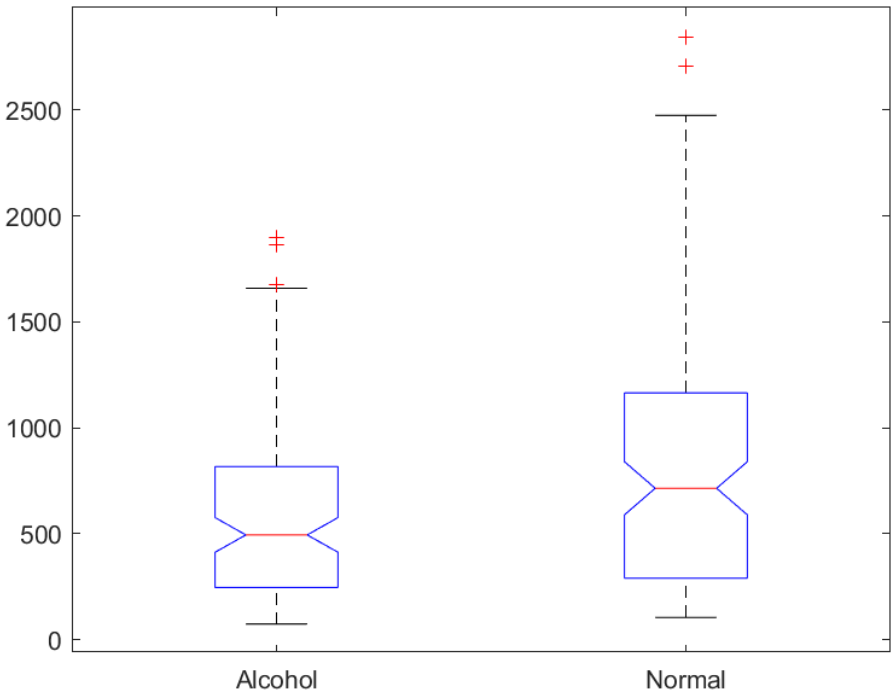

Fig. 3.3.13. WAVELEN SB13 KW test plot.

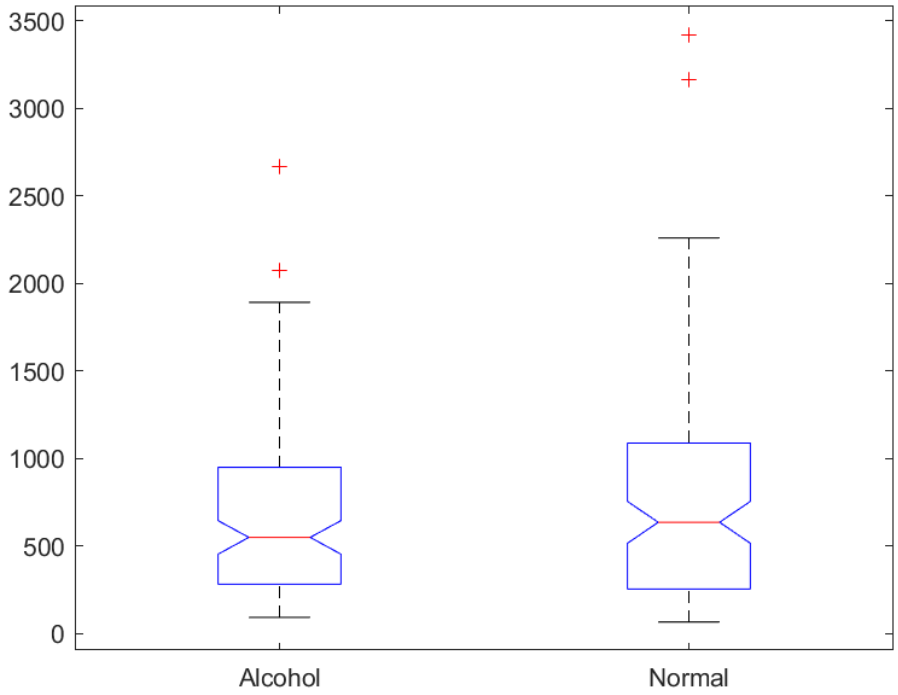

Fig. 3.3.14. WAVELEN SB14 KW test plot.

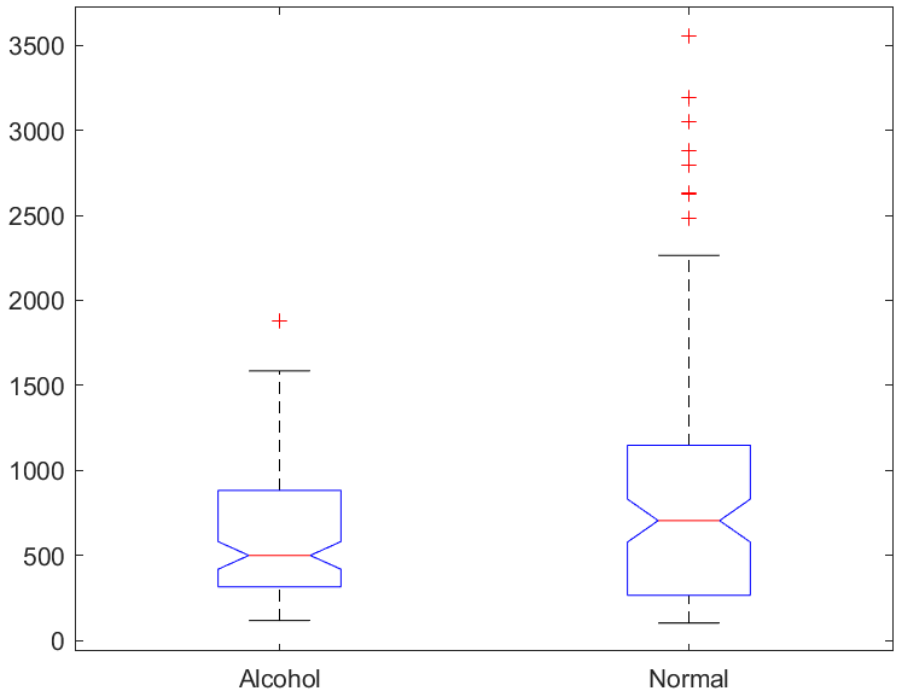

Fig. 3.3.15. WAVELEN SB15 KW test plot.

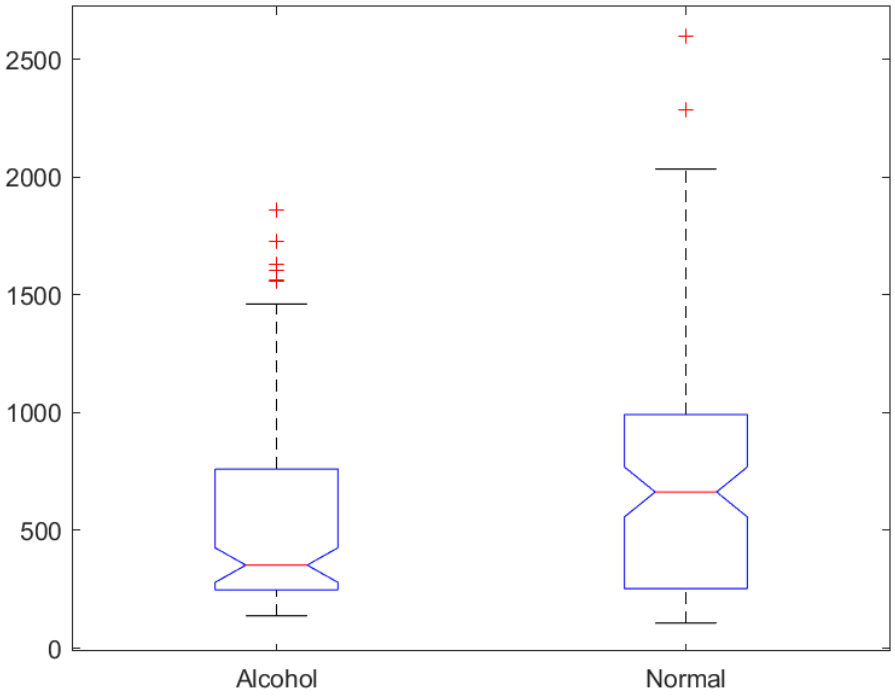

Fig. 3.3.16. WAVELEN SB16 KW test plot.

Subbands	IQR	WAVELEN
SB1	0.0293	0.5936
SB2	2.88×10^{-8}	7.85×10^{-12}
SB3	0.1033	0.0065
SB4	2.20×10^{-3}	2.51×10^{-10}
SB5	0.0635	0.0008
SB6	2.20×10^{-3}	4.31×10^{-10}
SB7	0.0046	3.34×10^{-6}
SB8	2.90×10^{-3}	2.42×10^{-7}
SB9	9.37×10^{-6}	4.48×10^{-12}
SB10	1.12×10^{-5}	8.74×10^{-10}
SB11	8.66×10^{-5}	7×10^{-10}
SB12	1.53×10^{-2}	1.90×10^{-5}
SB13	6.87×10^{-2}	3.20×10^{-3}
SB14	9.23×10^{-1}	3.80×10^{-1}
SB15	1.64×10^{-1}	1.22×10^{-1}
SB16	2×10^{-4}	2.31×10^{-2}

Table 3.1: For different SB's, the KW test p values of IQR and WAVELEN features.

SVM classifier variants	Accuracy
L- SVM	90.0%
Q- SVM	89.2%
Cu- SVM	90.0%
F- Gaussian SVM	83.8%
M- Gaussian SVM	93.8%
C- Gaussian SVM	89.2%
Optimizable SVM	94.2%

Table 3.2: The accuracy of the proposed features using SVM classifier variants.

Here F is Fine, M is Medium, C is Coarse, L is Linear, Q is Quadratic, Cu is Cubic.

The minimum error classification (MEC) plot reduces the classification error rate at the classification stage. Fig. 3.4 shows the MEC plot. The observed and estimated MEC is plotted in the graph. The square block indicates the efficient point hyper parameter and circle shows the minimum error hyper parameter.

The receiver operating characteristics Curve (ROC) of the used features is shown in Fig. 3.6. The quality of the used features can be determined by the ROC using the threshold values which ranging [0, 1]. true positive (t_p) rate with false positive (f_p) rate is plotted in this graph. The area under the curve (AUC) achieved is 0.97 for optimizable SVM model.

The confusion matrix (CM) is a representation of the classification problems predicted outcome. The CM of proposed features is shown in Fig. 3.5. The predicted class is represented by the rows of the CM, while the target class is represented by the columns. Perfectly classified elements are represented in diagonal elements, the remaining elements are incorrectly classified. By the use of CM other performance measures such as accuracy (AC), sensitivity (S_{en}), specificity (S_{pe}), F1-score(F_1), and Matthew's correlation coefficient (M_{CC}) are also computed for the validation of proposed features. The performance metrics for the proposed feature are presented in Table 3.3. Table 3.3 explains that the suggested method's misclassification rate of 5.83% is much lower, indicating that both classes of EEG signals are correctly classified. The S_{en} of 91.67% and S_{pe} of 96.67% are almost near to the optimum values of S_{en} and S_{pe}. Precision and recall are defined by the F1-score composite. The F1-score for the suggested technique is 0.94, which is closer to its maximum value. The classification performance was evaluated using M_{CC}. The M_{CC} value attained by the proposed method is 88.44%, which is closer to the ideal value.

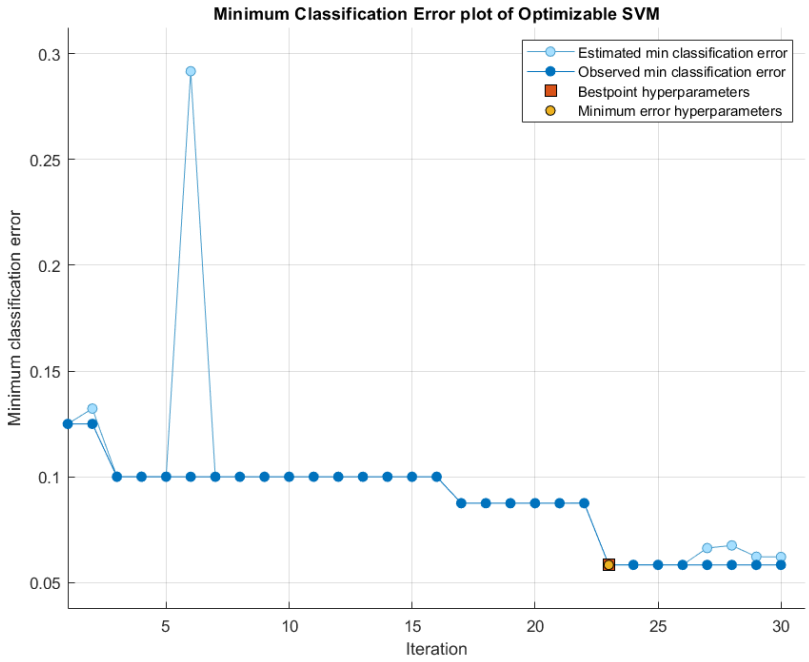

Fig. 3.4. MEC plot of optimizable SVM of the used features.

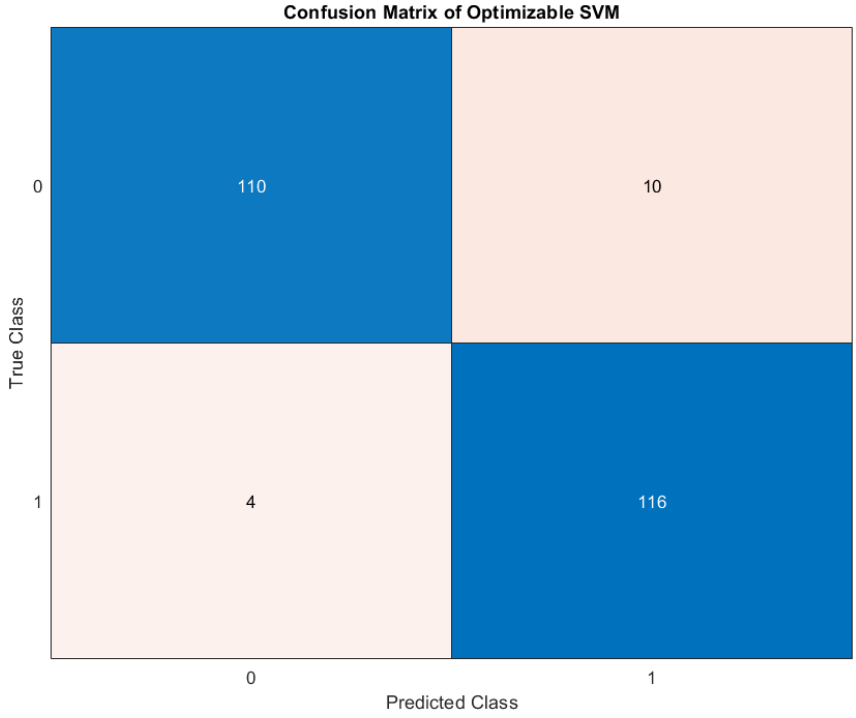

Fig. 3.5. Confusion Matrix of optimizable SVM of the used features.

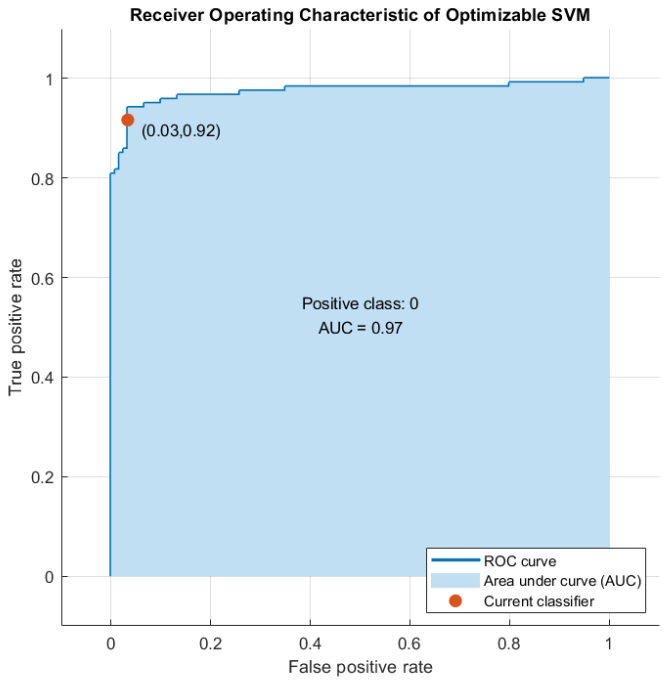

Fig. 3.6. ROC plot of optimizable SVM of the used features.

Performance measure (Ideal value)	Classification performance
AC (100%)	94.17
Error (0%)	5.83
S_{en} (100%)	91.67
S_{pe} (100%)	96.67
Precision (100%)	96.49
F_1 (1)	0.94
M_{CC} (100%)	88.44
Kappa (1)	0.88

Table 3.3: The suggested classification model's performance metrices.

The utility of the suggested strategy is now demonstrated by a comparison of performance utilizing the same dataset methods as shown in Table 3.4. The techniques are explored in terms of the classifier, and accuracy that have been achieved. Faust et al has achieved a significant ROC value of 0.822 using 9 features and using fuzzy

suggeno classifier (FSC) managed to achieve an accuracy of 92.4% [50, 63]. Ehlers et al has used DA for the classification and achieved an accuracy of 88% [59]. Acharya et al has managed to achieve an accuracy of 76.19% using SVM [65]. This table shows that present approaches use a variety of characteristics for the classification of alcohol and normal EEG data, which raises the classification complexity of an online classification system. The performance metrics S_{en}, S_{pe}, AC, and M_{CC} obtained by the suggested technique are 91.67%, 96.67%, 94.17%, and 88.44%, respectively. Such high classification accuracy demonstrates the method's dependability and resilience in classifying alcohol and normal EEG signals.

Author	Features	Classifier used	Classification performance (Average accuracy)
Faust et al [50]	PSD extraction, peak amplitude and frequency	ROC	0.822 (AUC)
Ehlers et al [59]	Correlation dimension	DA	88%
Acharya et al [65]	ApproxE, SaE, LE, HS	SVM with poly kernel	76.19%
Faust et al [63]	HOS cumulants	FSC	92.4%
Proposed method	IQR, Wavelength	Optimizable SVM	94.2%

Table 4: The suggested method's performance summary in comparison to existing techniques. Here SaE is sample-entropy, ApproxE is the approximate entropy, LE is Lyapunov-exponent, HS is higher-order spectra, FSC is fuzzy sugeno classifier.

3.5 Summary

This work presents the classification of the normal and alcohol EEG signals with the use of SSA. The KW test is used to perform the statistical analysis. Based on the KW test results the features are selected. The features used here are IQR and WAVELEN. The features are tested on optimize SVM for the selected subbands. The obtained classification accuracy is 94.17%, sensitivity is 91.67%, specificity is 96.67%

and precision is 96.49%. The suggested SSA based feature can be investigated for motor imagery tasks EEG signals classification, sleep apnea detection etc.

CHAPTER 4
Conclusion and Future Work

In this study the classification of EEG signals is explored using a signal processing in machine learning methods. The non-stationary technique-based features are introduced for the classification of various mental states EEG signals. Various features are extracted from the EEG signal. Based on the KW test probabilistic values the features are selected and are explored for the classification using machine learning algorithms. For the MI task classification FAWT technique-based features are introduced for the classification of focused, unfocussed and drowsiness mental states EEG signals. The LEE feature is explored for analyzing FAWT provided sub-bands. The KW test ensures the statistical significance of LEE feature. The LEE is computed from all sub-bands are tested on several machine learning techniques. The optimizable KNN provides the best classification as follows: accuracy is 93.25%, sensitivity is 91.38%, specificity is 96.24%, precision is 91.48%, the F1-score is 91.42%, and kappa value is 0.8481. The obtained results have better approximation when compared with the existing studies.

For the identification of alcoholic EEG signals, SSA based features are explored. The statistically significant feature subbands are selected and are fed to the machine learning algorithms. The features used here are IQR and WAVELEN. The features are tested on optimize SVM for the selected subbands. The obtained classification accuracy is 94.17%, sensitivity is 91.67%, specificity is 96.67% and precision is 96.49%.

The proposed work has the better results in comparison to the existing studies. The proposed approach can be explored in clinical based application for detecting different neurological disorders and classification of other bio-medical signals. The suggested SSA based feature can be investigated for motor imagery tasks EEG signals classification, sleep apnea detection etc.

REFERENCES

[1] T. Nykopp, “Statistical modelling issues for the adaptive brain interface,” Helsinki University of, 2001.

[2] N. Kannathal, U. R. Acharya, C. M. Lim, and P. K. Sadasivan, “Characterization of EEG—A comparative study,” Computer Methods and Programs in Biomedicine, vol. 80, no. 1, pp. 17–23, Oct. 2005.

[3] “Experiment for Psychophysiological Interaction and Empathic Cognition for Human- Robot Cooperative Work (PsyIntEC).” [Online]. Available: http://www.bth.se/com/gsil_cognitive_neural_eng.nsf/pages/psyintec. [Accessed: 06- May-2012].

[4] K. S. Sri and J. C. Rajapakse, “Extracting EEG rhythms using ICA-R,” in IEEE International Joint Conference on Neural Networks, 2008. IJCNN 2008. (IEEE World Congress on Computational Intelligence), 2008, pp. 2133 –2138.

[5] D. S. Sanei and J. A. Chambers, EEG Signal Processing. John Wiley & Sons, 2007.

[6] W. V. Drongelen, Signal Processing for Neuroscientists: Introduction to the Analysis of Physiological Signals. Academic Press, 2007.

[7] P. J. Allen, O. Josephs, and R. Turner, “A Method for Removing Imaging Artifact from Continuous EEG Recorded during Functional MRI,” NeuroImage, vol. 12, no. 2, pp. 230–239, Aug. 2000.

[8] J. Malmivuo and R. Plonsey, Bioelectromagnetism: Principles and Applications of Bioelectric and Biomagnetic Fields. Oxford University Press, 1995.

[9] S. Taran and V. Bajaj, "Sleep Apnea Detection Using Artificial Bee Colony Optimize Hermite Basis Functions for EEG Signals," in *IEEE Transactions on Instrumentation and Measurement*, vol. 69, no. 2, pp. 608-616, Feb. 2020.

[10] C. Neuper, G. R. M¨uller, A. K¨ubler, N. Birbaumer, G. Pfurtscheller, Clinical application of an eeg-based brain–computer interface: a case study in a patient with severe motor impairment, Clinical neurophysiology 114 (3) (2003) 399–409.

[11] A. R. Hassan, M. I. H. Bhuiyan, An automated method for sleep staging from eeg signals using normal inverse gaussian parameters and adaptive boosting, Neurocomputing 219 (2017) 76–87.

[12] A. R. Hassan, S. Siuly, Y. Zhang, Epileptic seizure detection in eeg signals using tunable-q factor wavelet transform and bootstrap aggregating, Computer methods and programs in biomedicine 137 (2016) 247–259.

[13]S. Taran, V. Bajaj, D. Sharma, S. Siuly, A. Sengur, Features based on analytic imf for classifying motor imagery eeg signals in bci applications, Measurement 116 (2018) 68–76.

[14]O. Aydemir, T. Kayikcioglu, Decision tree structure based classification of eeg signals recorded during two dimensional cursor movement imagery, Journal of neuroscience methods 229 (2014) 68–75.

[15]R. Zhang, X. Xiao, Z. Liu, W. Jiang, J. Li, Y. Cao, J. Ren, D. Jiang, L. Cui, A new motor imagery eeg classification method fb-trcsp+ rf based on csp and random forest, IEEE Access 6 (2018) 44944–44950.

[16]P. Herman, G. Prasad, T. M. McGinnity, D. Coyle, Comparative analysis of spectral approaches to feature extraction for eeg-based motor imagery classification, IEEE Transactions on Neural Systems and Rehabilitation Engineering 16 (4) (2008) 317–326.

[17]M. Spezialetti, L. Cinque, J. M. R. Tavares, G. Placidi, Towards eeg-based bci driven by emotions for addressing bci-illiteracy: a meta-analytic review, Behaviour & Information Technology 37 (8) (2018) 855–871.

[18]S. Bhattacharyya, A. Sengupta, T. Chakraborti, A. Konar, D. Tibarewala, Automatic feature selection of motor imagery eeg signals using differential evolution and learning automata, Medical & biological engineering & computing 52 (2) (2014) 131–139.

[19]G. Townsend, B. Graimann, G. Pfurtscheller, Continuous eeg classification during motor imagery-simulation of an asynchronous bci, IEEE Transactions on Neural Systems and Rehabilitation Engineering 12 (2) (2004) 258– 265.

[20]L. Qin, B. He, A wavelet-based time–frequency analysis approach for classification of motor imagery for brain–computer interface applications, Journal of neural engineering 2 (4) (2005) 65.

[21]S. Bhattacharyya, A. Khasnobish, S. Chatterjee, A. Konar, D. Tibarewala, Performance analysis of lda, qda and knn algorithms in left-right limb

movement classification from eeg data, in: 2010 International conference on systems in medicine and biology, IEEE, 2010, pp. 126–131.

[22]H. G¨oksu, Bci oriented eeg analysis using log energy entropy of wavelet packets, Biomedical Signal Processing and Control 44 (2018) 101–109.

[23]L. Duan, Z. Hongxin, M. S. Khan, M. Fang, Recognition of motor imagery tasks for bci using csp and chaotic pso twin svm, The Journal of China Universities of Posts and Telecommunications 24 (3) (2017) 83–90.

[24]Y. Sun, N. Ye, J. Yang, An asynchronous mi-bci system based on master-slave features, in: 2016 9th International Congress on Image and Signal Processing, BioMedical Engineering and Informatics (CISP-BMEI), IEEE, 2016, pp. 1456–1461.

[25]C. A. Stefano Filho, R. Attux, G. Castellano, Can graph metrics be used for eeg-bcis based on hand motor imagery?, Biomedical Signal Processing and Control 40 (2018) 359–365.

[26]Y. Zhang, C. S. Nam, G. Zhou, J. Jin, X. Wang, A. Cichocki, Temporally constrained sparse group spatial patterns for motor imagery bci, IEEE transactions on cybernetics 49 (9) (2018) 3322–3332.

[27]S. Saha, K. I. Ahmed, R. Mostafa, Wavelet coherence based channel selection for classifying single trial motor imagery, in: 2016 9th International Conference on Electrical and Computer Engineering (ICECE), IEEE, 2016, pp. 467–470.

[28]P. Gaur, R. B. Pachori, H. Wang, G. Prasad, A multi-class eeg-based bci classification using multivariate empirical mode decomposition based filtering and riemannian geometry, Expert Systems with Applications 95 (2018) 201–211.

[29]Y. Li, X. Li, M. Ratcliffe, L. Liu, Y. Qi, Q. Liu, A real-time eeg-based bci system for attention recognition in ubiquitous environment, in: Proceedings of 2011 international workshop on Ubiquitous affective awareness and intelligent interaction, 2011, pp. 33–40.

[30]A. Myrden, T. Chau, A passive eeg-bci for single-trial detection of changes in mental state, IEEE Transactions on neural systems and rehabilitation Engineering 25 (4) (2017) 345–356.

[31]Y. Ke, L. Chen, L. Fu, Y. Jia, P. Li, X. Zhao, H. Qi, P. Zhou, L. Zhang, B. Wan, et al., Visual attention recognition based on nonlinear dynamical

parameters of eeg, Bio-medical materials and engineering 24 (1) (2014) 349–355.

[32]N.-H. Liu, C.-Y. Chiang, H.-C. Chu, Recognizing the degree of human attention using eeg signals from mobile sensors, sensors 13 (8) (2013) 10273–10286.

[33]E. C. Djamal, H. Fadhilah, A. Najmurrokhman, A. Wulandari, F. Renaldi, Emotion brain-computer interface using wavelet and recurrent neural networks, International Journal of Advances in Intelligent Informatics 6 (1) (2020) 1–12.

[34]Y.-K. Wang, T.-P. Jung, C.-T. Lin, Eeg-based attention tracking during distracted driving, IEEE transactions on neural systems and rehabilitation engineering 23 (6) (2015) 1085–1094.

[35]Çiğdem İnan Acı, Murat Kaya, and Yuriy Mishchenko. 2019. Distinguishing mental attention states of humans via an EEG-based passive BCI using machine learning methods. Expert Syst. Appl. 134, C (Nov 2019), 153–166.

[36]S. K. Khare, V. Bajaj, A. Sengur, G. Sinha, Classification of mental states from rational dilation wavelet transform and bagged tree classifier using eeg signals, in: Artificial Intelligence-Based Brain-Computer Interface, Elsevier, 2022, pp. 217–235.

[37]S. Taran, V. Bajaj, Emotion recognition from single-channel eeg signals using a two-stage correlation and instantaneous frequency-based filtering method, Computer methods and programs in biomedicine 173 (2019) 157– 165.

[38]I. Bayram, An analytic wavelet transform with a flexible time-frequency covering, IEEE Transactions on Signal Processing 61 (5) (2012) 1131–1142.

[39]S. Chaudhary, S. Taran, V. Bajaj, S. Siuly, A flexible analytic wavelet transform based approach for motor-imagery tasks classification in bci applications, Computer Methods and Programs in Biomedicine 187 (2020) 105325.

[40]S. Aydın, H. M. Saraoˇglu, S. Kara, Log energy entropy-based eeg classification with multilayer neural networks in seizure, Annals of biomedical engineering 37 (12) (2009) 2626–2630.

[41]M. Rashid, N. Sulaiman, A. PP Abdul Majeed, R. M. Musa, B. S. Bari, S. Khatun, et al., Current status, challenges, and possible solutions of eeg based

brain-computer interface: a comprehensive review, Frontiers in neurorobotics (2020) 25.

[42]A. S. M. Miah, S. R. A. Ahmed, M. R. Ahmed, O. Bayat, A. D. Duru, M. K. I. Molla, Motor-imagery bci task classification using riemannian geometry and averaging with mean absolute deviation, in: 2019 Scientific Meeting on Electrical-Electronics & Biomedical Engineering and Computer Science (EBBT), Ieee, 2019, pp. 1–7.

[43]A. Phinyomark, P. Phukpattaranont, C. Limsakul, Feature reduction and selection for emg signal classification, Expert systems with applications 39 (8) (2012) 7420–7431.

[44]Rangaswamy, M., Jones, K.A., Porjesz, B., et al.: "Delta and theta oscillations as risk markers in adolescent offspring of alcoholics", Int. J. Psychophysiol., 63, (1), pp. 3–15, 2007.

[45]World health organization: 'Alcohol fact sheet number 349',2011, inverse gaussian parameters and adaptive boosting, Neurocomputing.

[46]Organization WH et al, "Global status report on alcohol", 2004.

[47]Druesne-Pecollo N, Tehard B, Mallet Y, Gerber M, Norat T, Hercberg S, Latino-Martel P, "Alcohol and genetic polymorphisms: effect on risk of alcohol-related cancer". Lancet Oncol 10(2):173–180, 2009.

[48]Faust O, Acharya R, Allen AR, Lin C, "Analysis of eeg signals during epileptic and alcoholic states using ar modeling techniques". IRBM 29(1):44–52, 2008.

[49]S. Taran, V. Bajaj, D. Sharma, S. Siuly, A. Sengur, Features based on analytic IMF for classifying motor imagery EEG signals in BCI applications, Measurement (2017).

[50]Nilima Salankar, Saeed Mian Qaisar, Paweł Pławiak, Ryszard Tadeusiewicz, Mohamed Hammad, EEG based alcoholism detection by oscillatory modes decomposition second order difference plots and machine learning, Biocybernetics and Biomedical Engineering, Volume 42, Issue 1, 2022, pp. 173-186, ISSN 0208-5216.

[51]Sharma, M., Deb, D. & Acharya, U.R. A novel three-band orthogonal wavelet filter bank method for an automated identification of alcoholic EEG signals. Appl Intell 48, 1368–1378 (2018).

[52]Diykh, M., Abdulla, S., Oudah, A.Y., Marhoon, H.A., Siuly, S., 2021. A Novel Alcoholic EEG Signals Classification Approach Based on AdaBoost k-means

Coupled with Statistical Model, in: Siuly, S., Wang, H., Chen, L., Guo, Y., Xing, C. (Eds.), Health Information Science. Springer International Publishing, Cham, pp. 82–92.

[53]Bavkar, S., Iyer, B., Deosarkar, S., 2021. Optimal EEG channels selection for alcoholism screening using EMD domain statistical features and harmony search algorithm. Biocybernetics and Biomedical Engineering 41, 83–96.

[54]Gleb V. Tcheslavski; Fahrettin F. Gonen (2012). Alcoholism-related alterations in spectrum, coherence, and phase synchrony of topical electroencephalogram. , 42(4), 0–401.

[55]Cindy L. Ehlers, James Havstad, Dean Prichard, and James Theiler (1998). Low Doses of Ethanol Reduce Evidence for Nonlinear Structure in Brain Activity. The Journal of Neuroscience, 18(18), 7474–7486.

[56]Sachin Taran, Varun Bajaj, G.R. Sinha, Kemal Polat, Detection of sleep apnea events using electroencephalogram signals, Applied Acoustics, Volume 181, 2021, 108137, ISSN 0003-682X.

[57]Acharya, U.R., Sree, S.V., Chattopadhyay, S., et al.: 'Automated diagnosis of normal and alcoholic EEG signals', Int. J. Neural Syst., 2012, 22, (03), p. 1250011.

[58]Oliver Faust, Ratna Yanti, and Wenwei Yu (2013). Automated Detection of Alcohol Related Changes in Electroencephalograph Signals. Journal of Medical Imaging and Health Informatics, 3(2), 333–339.

[59]Oliver Faust, Wenwei Yu, Nahrizul Adib Kadri (2013). Computer-based identification of normal and alcoholic eeg signals using wavelet packets and energy measures. Journal of Mechanics in Medicine and Biology, 13(3), 1350033–.

[60]Bajaj, V., Guo, Y., Sengur, A. et al. A hybrid method based on time–frequency images for classification of alcohol and control EEG signals. Neural Comput & Applic 28, 3717–3723 (2017).

[61]Shivnarayan Patidar, Ram Bilas Pachori, Abhay Upadhyay, U. Rajendra Acharya (2016). An integrated alcoholic index using tunable-Q wavelet transform based features extracted from EEG signals for diagnosis of alcoholism. Applied Soft Computing, (), S1568494616305713–.

[62]T.K. Padma Shri, N. Sriraam (2016). Spectral entropy feature subset selection using SEPCOR to detect alcoholic impact on gamma sub band visual event

related potentials of multichannel electroencephalograms (EEG). Applied Soft Computing, (), S1568494616301971–.

[63]Sachin Taran, Varun Bajaj, (2018). Rhythm-based identification of alcohol EEG signals. IET Science, Measurement & Technology, 12(3), 343–349.

[64]E. Malar, M. Gauthaam (2020). Wavelet analysis of EEG for the identification of alcoholics using probabilistic classifiers and neural networks. International Journal of Intelligence and Sustainable Computing, 1(1), 3–.

[65]Wu Di, Chen Zhihua, Feng Ruifang, Li Guangyu, Luan Tian (2010). [IEEE 2010 3rd IEEE International Conference on Computer Science and Information Technology (ICCSIT 2010) - Chengdu, China (2010.07.9-2010.07.11)] 2010 3rd International Conference on Computer Science and Information Technology - Study on human brain after consuming alcohol based on EEG signal. , (), 406–409.

[66]AshkanYazdani, S. Kamaledin Setarehdan (2007). [IEEE 2007 9th International Symposium on Signal Processing and Its Applications (ISSPA) - Sharjah, United Arab Emirates (2007.2.12-2007.2.15)] 2007 9th International Symposium on Signal Processing and Its Applications - Classification of EEG signals correlated with alcohol abusers. , (), 1–4.

[67]Nazari Kousarrizi, Mohammad Reza; Asadi Ghanbari, Abdolreza; Gharaviri, Ali; Teshnehlab, Mohammad; Aliyari, Mahdi (2009). [IEEE 2009 3rd International Conference on Bioinformatics and Biomedical Engineering (iCBBE) - Beijing, China (2009.06.11-2009.06.13)] 2009 3rd International Conference on Bioinformatics and Biomedical Engineering - Classification of Alcoholics and Non-Alcoholics via EEG Using SVM and Neural Networks. , (), 1–4.

[68]Manish Sharma, Pragya Sharma, Ram Bilas Pachori, U. Rajendra Acharya (2018). Dual-Tree Complex Wavelet Transform-Based Features for Automated Alcoholism Identification. International Journal of Fuzzy Systems, (), –.

[69]American Electroencephalographic Association 1990, Standard electrode position nomenclature, 2007. Available at http:/kdd.ics.uci.edu/databases/eeg/eeg.data.html/

[70]N. Golyandina, V. Nekrutkin, and A. Zhigljavsky, Analysis of time series structure: SSA and related techniques, ser. Monographs on statistics and applied probability. Boca Raton, Florida: Chapman and Hall, 2001, vol. 90.

[71]Sachin Taran, Prakash Chandra Sharma, Varun Bajaj, Automatic sleep stages classification using optimize flexible analytic wavelet transform, Knowledge-Based Systems, Volume 192, 2020, 105367, ISSN 0950-7051.

[72]Angkoon Phinyomark, Pornchai Phukpattaranont, Chusak Limsakul (2012). Feature reduction and selection for EMG signal classification. , 39(8), 7420–7431.

[73]Li, Shufang; Zhou, Weidong; Yuan, Qi; Geng, Shujuan; Cai, Dongmei (2013). Feature extraction and recognition of ictal EEG using EMD and SVM. Computers in Biology and Medicine, 43(7), 807–816.

[74]P. Jahankhani, V. Kodogiannis and K. Revett, "EEG Signal Classification Using Wavelet Feature Extraction and Neural Networks," *IEEE John Vincent Atanasoff 2006 International Symposium on Modern Computing (JVA'06)*, 2006, pp. 120-124, doi: 10.1109/JVA.2006.17.